splenic B-cells undergo somatic mutation, a genetic process strictly dependent on T-cell help [11]. Taken together, these features of ITP patients strongly suggest that antiplatelet autoantibody production is under the control of platelet-specific helper T-cells. Therefore, a detailed analysis of the T-cells autoreactive to platelet antigens is essential to understanding the pathogenic process in patients with ITP. This article focuses on the role of GPIIb-IIIa–reactive T-cells in the pathogenesis of ITP and particularly on how these autoreactive T-cells initiate and maintain pathogenic antiplatelet autoantibody production.

2. Characterization of GPIIb-IIIa–Reactive CD4+ T-Cells

The presence of T-cells autoreactive to platelets was first described by Semple and Freedman in 1991 [12]. In that report, they demonstrated that peripheral blood T-cells from ITP patients secreted interleukin 2 (IL-2) upon stimulation with autologous platelets. The production of IL-2 from circulating T-cells in response to platelets was further confirmed by Ware and Howard [13]. A subsequent study by Filion et al showed that this autoreactive T-cell response observed in ITP patients is the result of a breakdown in T-cell tolerance to platelet autoantigens in association with uncontrolled IL-2 expression [14]. In addition, Shimomura et al demonstrated an oligoclonal accumulation of CD4+ T-cells that frequently used the Vβ3, 6, 13.1, and 14 genes for their T-cell receptors in the peripheral blood of ITP patients [15]. These earlier studies together indicated that platelet antigen–reactive T-cells are expanded during and are associated with the pathogenic processes of ITP. However, the antigenic specificity of these platelet-reactive T-cells and whether they stimulated antiplatelet autoantibody production remained unclear.

In 1998, we found that GPIIb-IIIa is one of the major target antigens recognized by platelet-reactive CD4+ T-cells in ITP patients [16]. In that study, human GPIIb-IIIa affinity-purified from outdated platelet concentrates was used to examine antigen-specific T-cell responses, but peripheral blood T-cells from ITP patients and healthy individuals were virtually unresponsive to GPIIb-IIIa in its native form. Previous studies in our laboratory had indicated that structural modification of autoantigens could induce the expression of antigenic self-determinants that were recognized by pathogenic autoreactive T-cells in other autoimmune diseases [17,18]. With this result in mind, we prepared disulfide-reduced GPIIb-IIIa and tryptic peptides of GPIIb-IIIa and used them to stimulate T-cells. Using this system, we reproducibly detected T-cell proliferative responses induced by modified GPIIb-IIIa from the majority of ITP patients. We confirmed the specificity of the T-cell response by specifically activating T-cells primed with modified GPIIb-IIIa by means of recombinant GPIIb-IIIa fragments expressed in *Escherichia coli* in secondary cultures. A major proportion of the GPIIb-IIIa–reactive T-cells had a CD4+ helper phenotype and were restricted by HLA-DR. However, an in vitro T-cell proliferative response to chemically modified GPIIb-IIIa was also detected in many healthy individuals.

To evaluate the ability of GPIIb-IIIa–reactive CD4+ T-cells to stimulate antiplatelet autoantibody production, we set up an in vitro culture system in which peripheral blood T-and B-cells were cultured in the presence or absence of modified GPIIb-IIIa and the IgG anti–GPIIb-IIIa antibody levels were subsequently measured in the culture supernatants. IgG anti–GPIIb-IIIa antibodies were detected in the supernatants of ITP patients in an antigen-dependent manner but not in the supernatants of healthy individuals who showed T-cell proliferation induced by modified GPIIb-IIIa. This result is analogous to the in vitro production of antiphospholipid antibodies in peripheral blood mononuclear cell cultures from APS patients versus healthy individuals in response to a major autoantigen, β_2-glycoprotein I [18]. The difference between ITP patients and healthy individuals in the autoantibody response can be explained by a mechanism in which circulating memory B-cells capable of producing IgG autoantibodies are present in the patients but absent in healthy individuals [19]. This antibody production was inhibited specifically by a monoclonal antibody (MoAb) to HLA-DR, indicating a requirement for T-cell recognition of the antigen during the T-cell–B-cell interaction [16]. The IgG anti–GPIIb-IIIa antibodies produced in the in vitro cultures potentially act as antiplatelet antibodies in vivo in ITP patients because they are capable of binding to normal platelet surfaces (Figure 1). Therefore, it is likely that the GPIIb-IIIa–reactive T-cells detected in our assay are involved in the production of pathogenic antiplatelet antibodies in ITP patients.

To map the T-cell epitopes on GPIIb-IIIa, we examined the T-cell responses to 6 recombinant fragments covering different portions of GPIIbα and GPIIIa [20]. Peripheral blood T-cells from ITP patients and healthy individuals proliferated in response to the recombinant fragments in various combinations but frequently recognized the amino-terminal portions of both GPIIbα (amino acid residues 18-259) and GPIIIa (amino acid residues 22-262). More importantly, these amino-terminal fragments also stimulated the production of antiplatelet antibodies from autologous B-cells. When GPIIb-IIIa–reactive T-cell lines were generated from ITP patients by the repeated stimulation of peripheral blood T-cells with tryptic peptides of GPIIb-IIIa, most of the specific T-cell lines recognized the amino-terminal portion of GPIIbα or GPIIIa. From these findings, the amino-terminal portion of GPIIb-IIIa was deemed to be primarily responsible for the stimulation of autoreactive T-cells and subsequent autoantibody production. Notably, the antiplatelet autoantibodies in ITP patients mainly recognize the conformational epitope consisting of the amino-terminal portion of GPIIbα as well [9]. A study to finely map T-cell epitopes has been underway in our laboratory, but many epitopes appear to be associated with different HLA class II alleles, even in the amino-terminal portion of GPIIb-IIIa. On the other hand, Semple and coworkers showed that a synthetic peptide corresponding to amino acid residues 496 to 510 of GPIIIa stimulated IL-2 production in T-cell lines generated from the ITP spleen [21]. Moreover, another Japanese group reported that CD4+ T-cell lines from an ITP patient produced interferon γ (IFN-γ) in response to stimulation with a synthetic peptide consisting of GPIbα amino acid residues 429 to 443; this region contains anchor motifs for HLA-DRB1*0405 [22]. Interestingly, these T-cell lines also responded to autologous

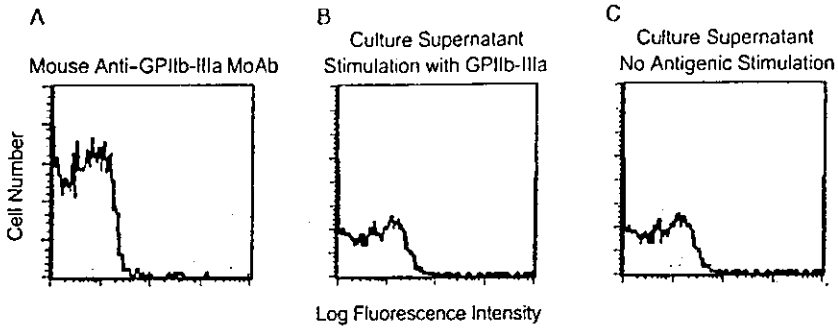

Figure 1. Binding of immunoglobulins in peripheral blood mononuclear cell (PBMC) culture supernatants to platelet surfaces. Platelets derived from healthy individuals were incubated with fluorescein-5-isothiocyanate (FITC)-conjugated mouse anti-glycoprotein IIb-IIIa (GPIIb-IIIa) monoclonal antibody (MoAb) (A). Platelets were also incubated with ITP patient-derived PBMC culture supernatants with (B) or without (C) antigenic stimulation with modified GPIIb-IIIa and then incubated with FITC-conjugated goat antihuman immunoglobulin G $F(ab')_2$ fragment. Cell staining analyzed by flow cytometry is shown as shaded histograms. Open histograms represent controls stained with FITC-conjugated isotype-matched MoAb to an irrelevant antigen (A) or with secondary antibody alone (B and C). Results shown are representative of 5 experiments using 4 different PBMC samples.

dendritic cells preincubated with platelet lysate. However, it is not known whether these T-cells, which are responsive to epitopes located in the center of GPIIbα and GPIIIa, can induce antiplatelet autoantibody production. These findings taken together indicated that T-cell epitopes are present throughout the GPIIbα and GPIIIa molecules, suggesting that the entire GPIIb-IIIa molecule is a target of the autoimmune response. In addition, these different results may reflect the heterogeneity of the T-cell response to GPIIb-IIIa in ITP patients.

$CD4^+$ helper T-cells are functionally classified according to their cytokine expression profiles. In this regard, several reports on serum T-cell–derived cytokines in ITP patients describe a helper T-cell subtype 1 (Th1) response or a mixed Th0/Th1 response [23,24]. We have generated more than 50 T-cell lines responsive to GPIIb-IIIa from the peripheral blood or spleen of ITP patients and have found that all of these T-cell lines produced IFN-γ and had a Th1- or Th0-like cytokine expression profile. In addition, IL-6 expression by these T-cell lines correlated with their ability to provide help to B-cells. It is now known that the Th1/Th2 antagonism in humans is not as strict as it is reported to be in mice, and T-cell function is associated with individual cytokine profiles rather than with the Th1/Th2 phenotype. Therefore, we further examined the roles of individual cytokines in regulating the production of anti–GPIIb-IIIa antibodies by using an in vitro assay system consisting of GPIIb-IIIa–reactive $CD4^+$ T-cell lines and autologous peripheral blood B-cells [20]. In this assay system, an anti–IL-6 MoAb blocked the T-cell–dependent production of anti–GPIIb-IIIa antibodies, but anti–IFN-γ and anti–IL-4 MoAbs did not, supporting the idea that IL-6 is the major B-cell–activating factor produced by GPIIb-IIIa–reactive $CD4^+$ T-cells. On the other hand, an anti-CD154 MoAb almost completely inhibited the in vitro production of anti–GPIIb-IIIa antibody induced by GPIIb-IIIa–reactive $CD4^+$ T-cell lines as well, indicating that CD40-CD154 engagement is also essential for the T-cell helper activity [25]. Taken together, these findings indicate that $CD4^+$ T-cell–dependent B-cell activation depends on 2 types of stimuli: T-cell–derived IL-6 and CD40-CD154 engagement.

$CD4^+$ T-cells that preferentially secrete transforming growth factor β1 (TGF-β1) are known to exert an immunosuppressive function through a bystander effect and are now called the *Th3 subset* [26]. In this regard, Andersson et al recently reported that ITP patients in remission had significantly elevated plasma levels of TGF-β1 [27], a finding later confirmed by Mouzaki et al [28]. Moreover, peripheral blood mononuclear cell cultures from ITP patients with active disease showed a reduced production of TGF-β1 [29]. Therefore, the T-cell cytokine profile is skewed toward a Th1/Th0 pattern in patients with active ITP and toward a Th3 response in patients in remission. This finding is potentially useful because the induction of platelet-reactive Th3 cells might be a therapeutic strategy for ITP. It is possible that the oral administration of autologous platelets induces platelet-specific tolerance through the induction of platelet antigen–reactive Th3 cells [30].

3. The Role of Cytotoxic T-Cells in ITP Pathogenesis

Earlier studies of the cell-mediated immune response in ITP patients considered cytotoxic platelet destruction as a possible pathogenic mechanism because a certain percentage of ITP patients do not have detectable antiplatelet antibodies [31]. Olsson et al recently demonstrated that the cell-mediated cytotoxic lysis of platelets by cytotoxic T-cells might contribute to thrombocytopenia in ITP [32]. In this study, a microarray analysis of peripheral blood T-cells revealed the increased expression of genes for ApoI/Fas, granzyme A, granzyme B, and perforin, together with Th1-related genes such as those for IFN-γ and IL-2 receptor, in ITP patients compared with healthy controls. An in vitro cytotoxicity assay showed the lysis of autologous platelets in patients with active ITP but not in patients in remission. In addition, ITP patients in remission showed increased gene and protein expression for several members of the killer cell immunoglobulin-like receptor family, which inhibit cytotoxic T-cells and natural killer cells. Currently, it is not known whether this phenomenon is mediated by the specific recognition of platelet antigens such as GPIIb-IIIa, by cytotoxic T-cells, or by the nonspecific activation of cytotoxic T-cells.

4. GPIIb-IIIa–Reactive T-Cells Recognize Cryptic Determinants

Circulating GPIIb-IIIa–reactive T-cells are detectable not only in ITP patients but also in many healthy individuals who do not have anti–GPIIb-IIIa antibodies [16,20], indicating that GPIIb-IIIa–reactive T-cells are a component of the normal T-cell repertoire. T-cells that recognize peptides generated from native GPIIb-IIIa by normal processing pathways are hypothesized to be deleted in the thymus through the process of "negative selection" because GPIIb-IIIa is expressed abundantly on thymic epithelial cells as early as the 16th week of intrauterine life [33]. However, Filion et al reported that $CD4^+$ T-cells reactive with liposome-encapsulated GPIIb-IIIa, which should have a native conformation, were detected in the peripheral blood from a majority of healthy individuals [34]. According to the report of Filion et al, the GPIIb-IIIa–reactive T-cells, which proliferated only in the presence of exogenous IL-2, did not produce their own IL-2 but expressed a high-affinity IL-2 receptor α on their surfaces. These features are consistent with the characteristics of anergic T-cells, which are T-cells in a functionally inactivated state after their antigenic stimulation in the periphery. Therefore, T-cell tolerance to GPIIb-IIIa is tightly maintained under normal circumstances. Some T-cells reactive to native GPIIb-IIIa escape thymic deletion and exist in the periphery; however, they are inactivated by a postthymic mechanism of peripheral tolerance [35].

To evaluate whether the GPIIb-IIIa–reactive T-cells in ITP patients are activated in vivo, we performed the following assays. First, the precursor frequency of GPIIb-IIIa–reactive T-cells in circulation was directly determined with limiting-dilution analysis [19]. The frequency of GPIIb-IIIa–reactive circulating T-cells was significantly increased in ITP patients, compared with healthy individuals. Second, the time course of the T-cell response to modified GPIIb-IIIa was evaluated by measuring the T-cell proliferative response on days 3, 5, 6, and 7 [16]. The T-cell response to modified GPIIb-IIIa in ITP patients was detectable on day 5 and peaked on day 6, whereas T-cells from healthy responders did not show the response on day 5 but did respond on day 7. These accelerated T-cell responses to modified GPIIb-IIIa in ITP patients indicate recent antigen exposure or the in vivo activation of such T-cells, whereas the kinetics of the T-cell responses induced by modified GPIIb-IIIa in healthy individuals were more typical of a naive T-cell response. Similar differences in the kinetics of autoantigen-specific T-cell proliferation in patients versus healthy individuals were shown for the T-cell responses to type II collagen in rheumatoid arthritis [36] and to topoisomerase I in scleroderma [37,38]. Taken together, these findings indicate that GPIIb-IIIa–reactive T-cells are activated in vivo in ITP patients but not in healthy individuals.

Because GPIIb-IIIa–reactive $CD4^+$ T-cells responded to the reduced GPIIb-IIIa or to tryptic peptides of GPIIb-IIIa but not to native GPIIb-IIIa complex [16], it is likely that the epitopes recognized by the GPIIb-IIIa–reactive T-cells are "cryptic" determinants. The concept of the cryptic self-determinant was initially proposed by Sercarz and colleagues [39,40] and has been extended by other investigators [41]. In this model, extracellular antigens are taken up by antigen-presenting cells (APCs) and degraded into peptide fragments by endosomal proteases (antigen-processing). Only the peptides with a capacity to bind HLA class II molecules are expressed on the cell surface and presented to T-cells. Of the numerous peptides predicted by the amino acid sequences of the autoantigen, a small proportion are presented to T-cells as a consequence of antigen processing and presentation. These peptides are representative of the autoantigen and termed *dominant self-determinants*, whereas the remaining peptides, which are not efficiently presented and are normally hidden from the immune system, are termed *cryptic self-determinants*. There is increasing interest in the possibility that crypticity is an important characteristic of the epitopes recognized by autoreactive T-cells and thus is relevant to autoimmune pathogenesis [41-43]. T-cells recognizing the dominant self-determinants in APCs undergo deletion in the thymus or inactivation in the periphery. On the other hand, T-cells specific for cryptic self-determinants are a component of the normal T-cell repertoire but normally do not encounter antigenic peptides in the periphery. These T-cells might become activated and autoaggressive if the previously cryptic self-determinants were presented at a higher concentration. Our findings regarding the T-cell response to GPIIb-IIIa in ITP patients are consistent with this cryptic epitope model because the GPIIb-IIIa–reactive T-cells recognize epitope peptides generated from structurally modified GPIIb-IIIa but not from native GPIIb-IIIa, exist in the normal T-cell repertoire, and are activated in vivo in ITP patients but not in healthy individuals.

5. Mechanisms for the Activation of GPIIb-IIIa–Reactive T-Cells

A fundamental question is how normally cryptic epitopes of platelet antigens such as GPIIb-IIIa become visible to the immune system and elicit a sustained pathogenic response in ITP patients. Because T-cells that are responsive to cryptic self-determinants would not encounter antigenic peptides in the periphery under normal circumstances, it is likely that a pathogenic autoreactive T-cell response is induced by the de novo presentation of a previously cryptic epitope under special conditions (Figure 2). To examine the mechanisms for activating GPIIb-IIIa–reactive T-cells in ITP patients, we sought to identify the site where GPIIb-IIIa–derived cryptic peptides are efficiently presented by APCs and subsequently induce the activation of GPIIb-IIIa–reactive T- and B-cells. The reticuloendothelial system, including the spleen, was a likely place because approximately 60% of ITP patients achieve a stable increased platelet count after surgical splenectomy [44] and because the spleen is considered the primary site of both platelet destruction and antiplatelet autoantibody production [45]. To test our hypothesis, we evaluated the frequencies and activation status of GPIIb-IIIa–reactive T- and B-cells in the peripheral blood and spleen obtained from ITP patients who had undergone splenectomy [19]. There were no differences in GPIIb-IIIa–reactive T-cell frequencies between the peripheral blood and spleen as determined by limiting-dilution analysis, but activated T-cells responsive to GPIIb-IIIa with accelerated proliferation rates and activated T-cells expressing CD154 were more frequent in the spleen than in the peripheral

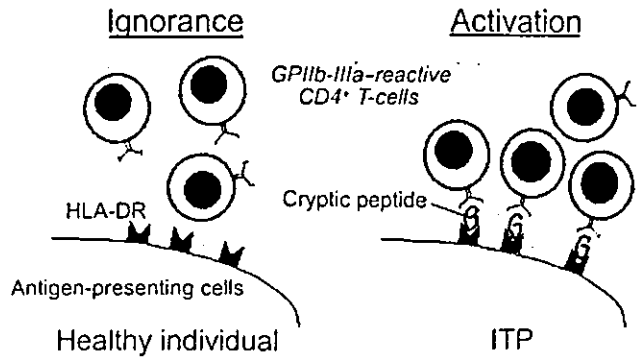

Figure 2. Activation of glycoprotein IIb-IIIa (GPIIb-IIIa)-reactive CD4⁺ T-cells in the normal T-cell repertoire by de novo presentation of a previously cryptic peptide of GPIIb-IIIa. T-cells recognizing a GPIIb-IIIa–derived cryptic peptide would not encounter the antigenic peptide in the periphery in healthy individuals (immunologic "ignorance"), whereas GPIIb-IIIa–reactive CD4⁺ T-cells are activated on recognition of the previously cryptic peptide expressed on functional antigen-presenting cells in patients with idiopathic thrombocytopenic purpura (ITP).

blood. The frequencies of B-cells producing anti-GPIIb-IIIa antibodies in the peripheral blood and spleen, as determined by enzyme-linked immunospot assay, were also similar; however, anti-GPIIb-IIIa antibodies were spontaneously produced by splenocytes in vitro but were scarcely secreted by peripheral blood mononuclear cells. CD19⁻/surface immunoglobulin–negative/CD38⁺/CD138⁺ plasma cells secreting anti-GPIIb-IIIa antibodies were detected exclusively in the spleen. Serial analysis showed that the frequencies of circulating GPIIb-IIIa–reactive T- and B-cells were markedly decreased after splenectomy in patients with a complete response but were unchanged in nonresponders. These findings indicated that the T-cell–B-cell interaction through recognition of the cryptic peptides of GPIIb-IIIa in ITP patients occurs primarily in the spleen. An increased delivery of antigen to the processing compartment is one of the potential mechanisms for revealing cryptic self-determinants in APCs [41], and splenic macrophages are likely to be primarily involved in this process. Splenic macrophages that phagocytose opsonized platelets via Fcγ receptors may have the ability to efficiently concentrate small quantities of platelet antigens that were previously cryptic. Taking these data into consideration leads us to propose a pathogenic loop that consists of antiplatelet autoantibody production by B-cells, phagocytosis of opsonized platelets and presentation of GPIIb-IIIa–derived cryptic peptides by splenic macrophages, and the exertion of helper activity by the GPIIb-IIIa–reactive CD4⁺ T-cells in ITP patients (Figure 3). Once this pathogenic loop is established, the antiplatelet autoantibody production is maintained endlessly. Therefore, therapeutic strategies for ITP should be aimed at interrupting this pathogenic cycle.

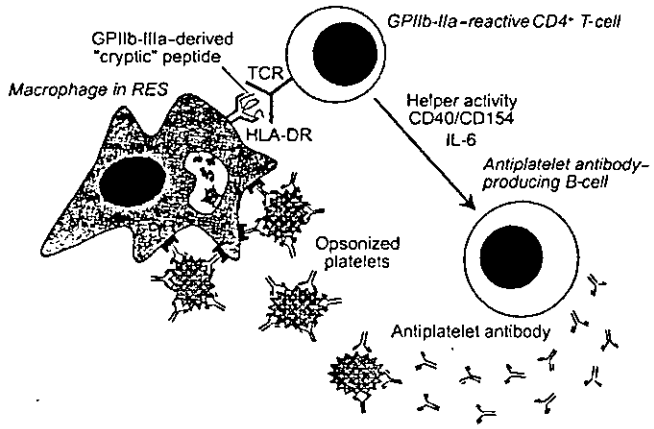

Figure 3. Schematic representation of a continuous pathogenic loop carried out by macrophages in the reticuloendothelial system (RES), glycoprotein IIb-IIIa (GPIIb-IIIa)-reactive CD4⁺ T-cells, and antiplatelet antibody–producing B-cells that maintain antiplatelet antibody production in patients with idiopathic thrombocytopenic purpura. A macrophage in the RES takes up opsonized platelets via the Fcγ receptor (FcγR) and presents a GPIIb-IIIa–derived cryptic peptide in the context of HLA-DR as a result of antigen processing. The GPIIb-IIIa–reactive CD4⁺ T-cell is activated by recognition of the HLA/cryptic peptide complex via the T-cell receptor (TCR). The activated GPIIb-IIIa–reactive CD4⁺ T-cell subsequently stimulates a specific B-cell to produce immunoglobulin G antiplatelet antibodies through the expression of CD154 and interleukin 6 (IL-6).

6. Potential Pathogenesis for ITP

In patients with ITP, macrophages in the reticuloendothelial system are a source of cryptic peptides that activate GPIIb-IIIa–reactive T- and B-cells. However, other mechanisms should contribute to the expression of cryptic peptides at the onset of the disease. It is difficult to identify those mechanisms by using samples from ITP patients because the triggering event may no longer be present in the patients (ie, a hit-and-run event). Figure 4 summarizes potential events that could induce the expression of cryptic epitopes derived from platelet antigens and the APCs that present the cryptic epitopes in the induction and chronic phases of ITP. Because determinant dominance during antigen processing in APCs is influenced by protein structure, conditions that change the molecular context of GPIIb-IIIa may permit the presentation of previously cryptic determinants, thereby breaking the

	Induction phase	Chronic phase
Magnitute of cryptic epitope expression	*Genetic disposition* *Nonspecific inflammation* *Suppressed regulatory function*	
Possible events	Infection of microorganism Drug/chemical exposure Massive destruction of platelets	Massive destruction of opsonized platelets
APC	Cross-reactive B-cell Dendritic cell/macrophage	Splenic macrophage

Figure 4. Potential events that induce the expression of cryptic epitopes of platelet antigens and the antigen-presenting cells (APCs) that present the cryptic epitopes in the induction and chronic phases of idiopathic thrombocytopenic purpura.

T-cell tolerance. Potential mechanisms for revealing cryptic self-determinants in APCs include the modulation of antigen processing, such as structural modification of self-antigens due to an unusual cleavage event or the formation of a complex with ligands that masks or unmasks cleavage sites for proteases in endosomes [41]. The factors that induce the expression of GPIIb-IIIa-derived cryptic peptides as a consequence of antigen processing in ITP patients are unknown, but several potential mechanisms can be proposed. For example, because chemical treatment of GPIIb-IIIa induces the expression of cryptic peptides that are recognized by T-cells, cryptic peptides may be revealed by chemical or drug exposure and a resultant structural modification. In this regard, patients taking D-penicillamine or gold salt sometimes develop a thrombocytopenia that is indistinguishable from ITP [46,47]. Alternatively, the complex of GPIIb-IIIa and its ligand may induce the expression of cryptic epitopes because fibrinogen and other GPIIb-IIIa–binding proteins have the Arg-Gly-Asp (RGD) sequence, and other unrelated proteins with the RGD sequence have been shown to bind GPIIb-IIIa [48]. In this regard, autoreactive T-cells and autoantibodies reportedly can be generated in normal mice by coimmunization with a mixture of self- and foreign antigens [49]. We recently found that β_2-glycoprotein I complexed with anionic phospholipids induces the expression of a cryptic epitope that is recognized by pathogenic autoreactive CD4$^+$ T-cells in APS patients [50].

Another potential mechanism is that ITP patients may have been exposed to foreign proteins that cross-react with GPIIb-IIIa. This mechanism is thought to involve the generation of cross-reactive B-cells that are initially primed by a foreign protein; they then bind a self-antigen and process and present self-peptides to T-cells [51]. Because B-cells that acquire antigen via surface immunoglobulin require approximately 1000 to 10,000 times less antigen for a subsequent T-cell response, B-cells may be able to efficiently concentrate small quantities of determinants that were previously cryptic [52]. In this regard, anti-GPIIIa antibodies in patients with human immunodeficiency virus (HIV)-related immune thrombocytopenia cross-react with HIV-associated gp120 [53]. The eradication of *Helicobacter pylori* from ITP patients was recently reported to induce a complete remission in nearly half of the patients [54]. The precise mechanism for this phenomenon remains unclear, but cross-reactivity between GPIIb-IIIa and the *H pylori* CagA protein has been proposed as a potential mechanism [55].

The efficient presentation of cryptic peptides derived from GPIIb-IIIa or other platelet antigens in APCs through one of the mechanisms described above would induce the activation of specific CD4$^+$ T-cells and the production of antiplatelet autoantibodies. However, to initiate the harmful autoimmune response requires additional factors, such as genetic disposition, nonspecific inflammation mediated by cytokines and toll-like receptor ligands, and/or suppressed regulatory function.

7. Summary and Future Perspectives

Accumulating evidence in the field of cellular immunity in ITP patients indicates an important role for platelet antigen–specific CD4$^+$ T-cells in antiplatelet antibody production and the pathogenesis of ITP. Further studies examining the mechanisms that induce the efficient presentation of cryptic T-cell determinants of platelet antigens as a consequence of antigen processing would clarify the etiology of ITP. In addition, the specific elimination or inactivation of pathogenic GPIIb-IIIa–reactive CD4$^+$ T-cells is a potential selective therapy for inhibiting the pathogenic antiplatelet antibody production in patients with ITP.

Acknowledgments

This work was supported by grants from the Japanese Ministry of Health, Welfare and Labor and the Japanese Ministry of Education, Science, Sports and Culture.

References

1. Cines DB, Blanchette VS. Immune thrombocytopenic purpura. *N Engl J Med.* 2002;346:995-1008.
2. McMillan R. Autoantibodies and autoantigens in chronic immune thrombocytopenic purpura. *Semin Hematol.* 2000;37:239-248.
3. He R, Reid DM, Jones CE, Shulman NR. Spectrum of Ig classes, specificities, and titers of serum antiglycoproteins in chronic idiopathic thrombocytopenic purpura. *Blood.* 1994;83:1024-1032.
4. Hürlmann-Forster M, Steiner B, von Felten A. Quantitation of platelet-specific autoantibodies in platelet eluates of ITP patients measured by a novel ELISA using purified glycoprotein complexes GPIIb/IIIa and GPIb/IX as antigens. *Br J Haematol.* 1997;98:328-335.
5. Kuwana M, Okazaki Y, Kaburaki J, Ikeda Y. Detection of circulating B cells secreting platelet-specific autoantibody is a sensitive and specific test for the diagnosis of autoimmune thrombocytopenia. *Am J Med.* 2003;114:322-325.
6. Mohan C, Adams S, Stanik V, Datta SK. Nucleosome: a major immunogen for pathogenic autoantibody-inducing T cells of lupus. *J Exp Med.* 1993;177:1367-1381.
7. Arai T, Yoshida K, Kaburaki J, et al. Autoreactive CD4$^+$ T-cell clones to β_2-glycoprotein I in patients with antiphospholipid syndrome: preferential recognition of the major phospholipid-binding site. *Blood.* 2001;98:1889-1896.
8. Fujisawa K, McMillan R. Platelet-associated antibody to glycoprotein IIb/IIIa from chronic immune thrombocytopenic purpura patients often binds to divalent cation-dependent antigens. *Blood.* 1993;81:1284-1289.
9. Kosugi S, Tomiyama Y, Honda S, et al. Platelet-associated anti-GPIIb-IIIa autoantibodies in chronic immune thrombocytopenic purpura recognizing epitopes close to the ligand-binding site of glycoprotein (GP) IIb. *Blood.* 2001;98:1819-1827.
10. Kuwana M, Kaburaki J, Pandey JP, et al. HLA class II alleles in Japanese patients with immune thrombocytopenic purpura: associations with anti-platelet glycoprotein antibodies and responses to splenectomy. *Tissue Antigens.* 2000;56:337-343.
11. Roark JH, Bussel JB, Cines DB, Siegel DL. Genetic analysis of autoantibodies in idiopathic thrombocytopenic purpura reveals evidence of clonal expansion and somatic mutation. *Blood.* 2002; 100:1388-1398.
12. Semple JW, Freedman J. Increased antiplatelet T helper lymphocyte reactivity in patients with autoimmune thrombocytopenia. *Blood.* 1991;78:2619-2625.
13. Ware RE, Howard TA. Phenotypic and clonal analysis of T lymphocytes in childhood immune thrombocytopenic purpura. *Blood.* 1993;82:2137-2142.
14. Filion MC, Bradley AJ, Devine DV, Decary F, Chartrand P. Autoreactive T cells in healthy individuals show tolerance in vitro with characteristics similar to but distinct from clonal anergy. *Eur J Immunol.* 1995;25:3123-3127.
15. Shimomura T, Fujimura K, Takafuta T, et al. Oligoclonal accumula-

tion of T cells in peripheral blood from patients with idiopathic thrombocytopenic purpura. *Br J Haematol.* 1996;95:732-737.
16. Kuwana M, Kaburaki J, Ikeda Y. Autoreactive T cells to platelet GPIIb-IIIa in immune thrombocytopenic purpura: role in production of anti-platelet autoantibody. *J Clin Invest.* 1998;102:1393-1402.
17. Kuwana M, Medsger TA Jr, Wright TM. Highly restricted TCR-αβ usage by autoreactive human T cell clones specific for DNA topoisomerase I: recognition of an immunodominant epitope. *J Immunol.* 1997;158:485-491.
18. Hattori N, Kuwana M, Kaburaki J, Mimori T, Ikeda Y, Kawakami Y. T cells that are autoreactive to β_2-glycoprotein I in patients with antiphospholipid syndrome and healthy individuals. *Arthritis Rheum.* 2000;43:65-75.
19. Kuwana M, Okazaki Y, Kaburaki J, Kawakami Y, Ikeda Y. Spleen is a primary site for activation of platelet-reactive T and B cells in patients with immune thrombocytopenic purpura. *J Immunol.* 2002;168:3675-3682.
20. Kuwana M, Kaburaki J, Kitasato H, et al. Immunodominant epitopes on glycoprotein IIb-IIIa recognized by autoreactive T cells in patients with immune thrombocytopenic purpura. *Blood.* 2001;98: 130-139.
21. Semple JW. Pathogenic T-cell responses in patients with autoimmune thrombocytopenic purpura. *J Pediatr Hematol Oncol.* 2003; 25(suppl 1):S11-S13.
22. Yamanouchi J, Hato T, Tamura T, Fujita S, Yasukawa M. Identification of an epitope on glycoprotein IIb-IIIa that is recognized by HLA-DRB1*0405-restricted CD4+'superior' T cells from a patient with immune thrombocytopenic purpura. *J Thromb Haemost.* 2004; 2:348-350.
23. Semple JW, Milev Y, Cosgrave D, et al. Differences in serum cytokine levels in acute and chronic autoimmune thrombocytopenic purpura: relationship to platelet phenotype and antiplatelet T-cell reactivity. *Blood.* 1996;87:4245-4254.
24. Panitsas FP, Theodoropoulou M, Kouraklis A, et al. Adult chronic idiopathic thrombocytopenic purpura (ITP) is the manifestation of a type-1 polarized immune response. *Blood.* 2004;103:2645-2647.
25. Kuwana M, Kawakami Y, Ikeda Y. Suppression of autoreactive T-cell response to glycoprotein IIb/IIIa by blockade of CD40/ CD154 interaction: implications for treatment of immune thrombocytopenic purpura. *Blood.* 2003;101:621-623.
26. Prud'homme GJ, Piccirillo CA. The inhibitory effects of transforming growth factor-β1 (TGF-β1) in autoimmune diseases. *J Autoimmun.* 2000;14:23-42.
27. Andersson PO, Stockelberg D, Jacobsson S, Wadenvik H. A transforming growth factor-β1-mediated bystander immune suppression could be associated with remission of chronic idiopathic thrombocytopenic purpura. *Ann Hematol.* 2000;79:507-513.
28. Mouzaki A, Theodoropoulou M, Gianakopoulos I, Vlaha V, Kyrtsonis MC, Maniatis A. Expression patterns of Th1 and Th2 cytokine genes in childhood idiopathic thrombocytopenic purpura (ITP) at presentation and their modulation by intravenous immunoglobulin G (IVIg) treatment: their role in prognosis. *Blood.* 2002;100: 1774-1779.
29. Andersson PO, Olsson A, Wadenvik H. Reduced transforming growth factor-β1 production by mononuclear cells from patients with active chronic idiopathic thrombocytopenic purpura. *Br J Haematol.* 2002;116:862-867.
30. Hermida G, Manjon R, Casanova F, Rodriguez-Salazar M. Oral vaccination with autologous platelets in chronic autoimmune thrombocytopenic purpura. *Med Hypotheses.* 2001;57:612-615.
31. Wybran J, Fudenberg HH. Cellular immunity to platelets in idiopathic thrombocytopenic purpura. *Blood.* 1972;40:856-861.
32. Olsson B, Andersson PO, Jernas M, et al. T-cell-mediated cytotoxicity toward platelets in chronic idiopathic thrombocytopenic purpura. *Nat Med.* 2003;9:1123-1124.
33. Gruel Y, Boizard B, Daffos F, Forestier F, Caen J, Wautier JL. Determination of platelet antigens and glycoproteins in the human fetus. *Blood.* 1986;68:488-492.
34. Filion MC, Proulx C, Bradley AJ, et al. Presence in peripheral blood of healthy individuals of autoreactive T cells to a membrane antigen present on bone marrow-derived cells. *Blood.* 1996;88: 2144-2150.
35. Lo D, Freedman J, Hesse S, Brinster RL, Sherman L. Peripheral tolerance in transgenic mice: tolerance to class II MHC and non-MHC transgene antigens. *Immunol Rev.* 1991;122:87-102.
36. Snowden N, Reynolds I, Morgan K, Holt L. T cell responses to human type II collagen in patients with rheumatoid arthritis and healthy controls. *Arthritis Rheum.* 1997;40:1210-1218.
37. Kuwana M, Medsger TA Jr, Wright TM. T cell proliferative response induced by DNA topoisomerase I in patients with systemic sclerosis and healthy donors. *J Clin Invest.* 1995;96:586-596.
38. Kuwana M, Feghali CA, Medsger TA Jr, Wright TM. Autoreactive T cells to topoisomerase I in monozygotic twins discordant for systemic sclerosis. *Arthritis Rheum.* 2001;44:1654-1659.
39. Lehmann PV, Forsthuber T, Miller A, Sercarz EE. Spreading of T-cell autoimmunity to cryptic determinants of an autoantigen. *Nature.* 1992;358:155-157.
40. Sercarz EE, Lehmann PV, Ametani A, Benichou G, Miller A, Moudgil K. Dominance and crypticity of T cell antigenic determinants. *Annu Rev Immunol.* 1993;11:729-766.
41. Lanzavecchia A. How can cryptic epitopes trigger autoimmunity? *J Exp Med.* 1995;181:1945-1948.
42. Warnock MG, Goodacre JA. Cryptic T-cell epitopes and their role in the pathogenesis of autoimmune diseases. *Br J Rheumatol.* 1997; 36:1144-1150.
43. Kuwana M. β_2-glycoprotein I: antiphospholipid syndrome and T-cell reactivity. *Thromb Res.* 2004;114:347-355.
44. Stasi R, Stipa E, Masi M, et al. Long-term observation of 208 adults with chronic idiopathic thrombocytopenic purpura. *Am J Med.* 1995;98:436-442.
45. Sandler SG. The spleen and splenectomy in chronic immune (idiopathic) thrombocytopenic purpura. *Semin Hematol.* 2000; 37(suppl 1):10-12.
46. Stein HB, Patterson AC, Offer RC, Atkins CJ, Teufel A, Robinson HS. Adverse effects of D-penicillamine in rheumatoid arthritis. *Ann Intern Med.* 1980;92:24-29.
47. Garner SF, Campbell K, Metcalfe P, et al. Glycoprotein V: the predominant target antigen in gold-induced autoimmune thrombocytopenia. *Blood.* 2002;100:344-346.
48. Lazarus R, McDowell RS. Structural and functional aspects of RDG-containing protein antagonists of glycoprotein IIb-IIIa. *Curr Opin Biotechnol.* 1993;4:438-445.
49. Dong X, Hamilton KJ, Satoh M, Wang J, Reeves WH. Initiation of autoimmunity to the p53 tumor suppressor protein by complexes of p53 and SV40 large T antigen. *J Exp Med.* 1994;179:1243-1252.
50. Kuwana M, Matsuura E, Kobayashi K, et al. Binding of β_2-glycoprotein I to anionic phospholipids facilitates processing and presentation of a cryptic epitope that activates pathogenic autoreactive T cells. *Blood.* 2005. In press.
51. Mamula MJ, Fatenejad S, Craft J. B cells process and present lupus autoantigens that initiate autoimmune T cell responses. *J Immunol.* 1994;152:1453-1461.
52. Mamula MJ, Janeway CA Jr. Do B cells drive the diversification of immune responses? *Immunol Today.* 1993;14:151-152.
53. Bettaieb A, Oksenhendler E, Duedari N, Bierling P. Cross-reactive antibodies between HIV-gp120 and platelet gpIIIa (CD61) in HIV-related immune thrombocytopenic purpura. *Clin Exp Immunol.* 1996;103:19-23.
54. Franchini M, Veneri D. *Helicobacter pylori* infection and immune thrombocytopenic purpura: an update. *Helicobacter.* 2004;9:342-346.
55. Takahashi T, Yujiri T, Shinohara K, et al. Molecular mimicry by *Helicobacter pylori* CagA protein may be involved in the pathogenesis of *H. pylori*-associated chronic idiopathic thrombocytopenic purpura. *Br J Haematol.* 2004;124:91-96.

Genetic Defects Leading to Hereditary Thrombotic Thrombocytopenic Purpura

Koichi Kokame and Toshiyuki Miyata

In patients with thrombotic thrombocytopenic purpura (TTP), unusually large multimers of von Willebrand factor (VWF) circulate in the plasma. This is caused by a functional deficiency of VWF-cleaving protease, ADAMTS-13. Although TTP usually occurs as an acquired form due to autoantibodies against ADAMTS-13, the condition may be inherited in an autosomal recessive fashion. Thus far, genomic DNA from 23 patients with hereditary TTP and their families has been analyzed and 33 causative mutations identified in the *ADAMTS13* gene: 19 missense, five nonsense, five frameshift, and four splice mutations. Common missense polymorphisms have been also found, one of which significantly reduces ADAMTS-13 activity. No cases have been found without mutations in the *ADAMTS13* gene, suggesting that genetic defects in *ADAMTS13* are the dominant cause of hereditary TTP. Further analysis may reveal the genetic background associated with acquired TTP and other thrombotic diseases.

THROMBOTIC thrombocytopenic purpura (TTP) is a highly lethal disease characterized by five features: thrombocytopenia, microangiopathic hemolytic anemia, renal failure, fever, and neurological dysfunction.[1] In TTP, platelet thrombi form within the microvasculature, which is thought to be caused by accumulation of unusually large multimers of von Willebrand factor (VWF). The majority of TTP is acquired, often affecting adolescents and adults. In a smaller number of cases, TTP is inherited in an autosomal recessive fashion, and hereditary TTP with neonatal onset and frequent relapses is often diagnosed as Upshaw-Schulman syndrome.[2]

VWF is synthesized primarily in vascular endothelial cells and secreted into the plasma as large multimeric forms.[3-6] Normally, the large multimers are cleaved into smaller forms by a plasma metalloprotease, ADAMTS-13,[7-11] which is a member of the ADAMTS (a disintegrin-like and metalloprotease [reprolysin type] with thrombospondin type 1 motif) gene family. In acquired TTP, autoantibodies against ADAMTS-13 are produced that inhibit the VWF-cleaving activity of ADAMTS-13, leading to the accumulation of highly active large VWF multimers.[12,13] In contrast, patients with hereditary TTP innately have no plasma ADAMTS-13 activity. Thus far, 33 causative mutations have been identified in the *ADAMTS13* gene and here we summarize the genetic defects leading to hereditary TTP. We describe the gene symbol of ADAMTS-13 as *ADAMTS13*, according to gene nomenclature provided by the Human Gene Nomenclature Committee. We refer to the protein as ADAMTS-13 according to recommendation of Dr Suneel S. Apte (http://www.lerner.ccf.org/bme/apte/adamts/nomenclature.php).

Structural Properties of ADAMTS-13

Human ADAMTS-13 was purified from plasma[14-16] and its cDNA was cloned.[16-18] At the same time, *ADAMTS13* was also identified as the responsible gene for hereditary TTP by linkage analysis.[19] ADAMTS-13 consists of 1,427 amino acid residues, containing an N-terminal signal peptide, a propeptide, a reprolysin-like metalloprotease domain, a disintegrin-like domain, a thrombospondin type-1 motif (TSP1), a cysteine-rich domain, a spacer domain, seven additional TSP1 repeats, and two CUB domains (Fig 1). Its mRNA is predominantly expressed in liver.[16,17,19,20]

Functional Properties of ADAMTS-13

The only known physiological substrate of ADAMTS-13 is VWF multimers, which play a pivotal role in platelet aggregation. ADAMTS-13 specifically cleaves the peptidyl bond between Y1605 and M1606 in the VWF A2 domain.[21-24] Systematic studies on the structure and function of ADAMTS-13, using recombinant ADAMTS-13 with progressive C-terminal truncations, determined the domains required for

From the National Cardiovascular Center Research Institute, Osaka, Japan.
Supported in part by grants-in-aid from the Ministry of Health, Labour, and Welfare of Japan, and from the Ministry of Education, Culture, Sports, Science, and Technology of Japan.
Address correspondence to Toshiyuki Miyata, PhD, National Cardiovascular Center Research Institute, 5-7-1 Fujishirodai, Suita, Osaka 565-8565, Japan.

0037-1963/04/4101-0002$30.00/0
doi:10.1053/j.seminhematol.2003.10.002

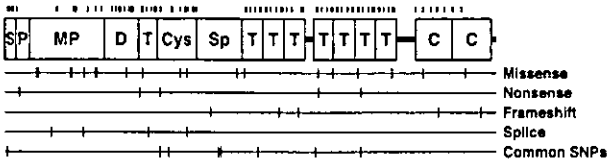

Figure 1. ADAMTS-13 mutations. The mutated sites responsible for hereditary TTP and common SNPs are shown below the domain structures of human ADAMTS-13. All cysteine residues are shown above. S, signal peptide; P, propeptide; MP, metalloprotease domain; D, disintegrin-like domain; T, TSP1 motif; Cys, cysteine-rich domain; Sp, spacer domain; C, CUB domain.

VWF cleavage.[25,26] Enzymatic analysis of these mutants showed that removal of the cysteine-rich/spacer domains caused loss of proteolytic activity towards VWF. The more C-terminal TSP1 and CUB domains were dispensable for VWF-cleaving activity, at least in vitro.

Thirty-three Mutations Responsible for TTP

To date, 33 mutations responsible for hereditary TTP have been identified in the *ADAMTS13* gene[19,27-30] (Table 1 and Fig 1). Five result in frameshift deletions or insertions and four are splice mutations. The remaining 24 mutations lead to codon changes, 19 of which are nonconservative missense and five of which are nonsense mutations. The mutated sites in *ADAMTS13* are distributed across many exons and introns throughout the gene, which spans approximately 37 kb on chromosome 9q34. The absence of clusters of mutations within the metalloprotease domain implies structural and functional importance of other regions.

Missense Mutations

Nineteen missense mutations have been identified: H96D, R102C, R193W, T196I, L232Q, S263C, R268P, P353L, R398H, C508Y, R528G, I673F, R692C, C908Y, C951G, C1024G, R1123C, C1213Y, and R1336W. Nine mutations are substitutions to/from cysteine residues, suggesting that disulfide-bond formation is important for proper conformation and function.

Among these, only six mutations were characterized by expression analysis.[27,31] We made mammalian expression plasmids for the R193W, R268P, C508Y, I673W, C908Y, and R1123C mutants, as well as wild-type ADAMTS-13, and then transfected them into cultured HeLa cells. A FLAG-tag sequence was added to the C terminus to aid in immunochemical detection. Transient expression of wild-type ADAMTS-13 produced a single immunoreactive band in culture medium, whereas none of the mutants were secreted, except for the R193W mutant, which was secreted at very low levels. Therefore, these six mutations must affect some aspect of the secretory pathway, possibly causing changes in protein folding and stability. The majority of the 19 identified missense mutations may cause secretory problems, similar to those in these five mutations.

Nonsense Mutations

Five nonsense mutations have been found: Q44X, W390X, Q449X, R910X, and R1034X. Among these, only one mutation, Q449X, was characterized by expression analysis.[26,27] The Q449X mutant was secreted efficiently like wild-type ADAMTS-13, but showed little cleavage activity towards VWF multimers.

As described above, the ADAMTS-13 spacer region is necessary for normal enzymatic activity. Since the W390X and Q449X mutants do not contain the spacer region, they would not possess VWF-cleaving activity, even if they are secreted. Alternatively, mRNAs derived from these nonsense mutant *ADAMTS13* genes may be destroyed by the nonsense-mediated decay (NMD) pathway (mRNA surveillance), which

Table 1. *ADAMTS13* Gene Mutations Responsible for Hereditary TTP

Exon/ Intron	Nucleotide	AA	Domain	Reference
Ex. 2	130C→T	Q44X	Propeptide	29
Ex. 3	286C→G	H96D	Metalloprotease	19
Ex. 3	304C→T	R102C	Metalloprotease	19
Int. 4	414+1G→A	Splice	Metalloprotease	31
Ex. 6	577C→T	R193W	Metalloprotease	31
Ex. 6	587C→T	T196I	Metalloprotease	19
Int. 6	686+1G→A	Splice	Metalloprotease	31
Ex. 7	695T→A	L232Q	Metalloprotease	28
Ex. 7	788C→G	S263C	Metalloprotease	28
Ex. 7	803G→C	R268P	Metalloprotease	27
Ex. 9	1058C→T	P353L	Disintegrin-like	28
Ex. 10	1169G→A	W390X	Tsp1-1	28
Ex. 10	1193G→A	R398H	Tsp1-1	19
Int. 10	1244+2T→G	Splice	Tsp1-1	31
Ex. 12	1345C→T	Q449X	Cysteine-rich	27
Ex. 13	1523G→A	C508Y	Cysteine-rich	27
Ex. 13	1582A→G	R528G	Cysteine-rich	19
Int. 13	1584+5G→A	Splice	Cysteine-rich	19
Ex. 15	1783delTT	Frameshift	Spacer	30
Ex. 17	2017A→T	I673F	Spacer	31
Ex. 17	2074C→T	R692C	Tsp1-2	19
Ex. 19	2376del26	Frameshift	Tsp1-3	19
Ex. 20	2549delAT	Frameshift	Tsp1-4	28
Ex. 21	2723G→A	C908Y	Tsp1-5	31
Ex. 21	2728C→T	R910X	Tsp1-5	28
Ex. 22	2851T→G	C951G	Tsp1-5	19
Ex. 24	3070T→G	C1024G	Tsp1-7	19
Ex. 24	3100A→T	R1034X	Tsp1-7	28
Ex. 25	3367C→T	R1123C	Tsp1-8	31
Ex. 26	3638G→A	C1213Y	CUB1	19
Ex. 27	3769insT	Frameshift	CUB1	19
Ex. 28	4006C→T	R1336W	CUB2	29
Ex. 29	4143insA	Frameshift	CUB2	28

Table 2. Mutated Alleles of Each Patient With Hereditary TTP

Patient	Allele 1	Allele 2	Reference
A1	R692C	R692C	9
A2	H96D	C951G	19
A3	R528G	Frameshift (3769insT)	19
A4	R398H	C1024G	19
A5	R102C	T196I	19
A6	Frameshift (2376del26)	C1213Y	19
A7	Splice (1584+5G→A)	ND	19
B1	R268P	C508Y	27
B2	Q449X	Q449X	27
C1	S263C	Frameshift (4143insA)	28
C2	P353L	R910X	28
C3	R1034X	Frameshift (4143insA)	28
C4	L232Q	L232Q	28
C5	W390X	Frameshift (2549delAT)	28
C6	P353L	Frameshift (4143insA)	28
C7	R910X	Frameshift (4143insA)	28
D1	Q44X	R1336W	29
E1	Frameshift (1783delTT)	Frameshift (1783delTT)	30
F1	Splice (414+1G→A)	Splice (414+1G→A)	31
F2	Splice (414+1G→A)	1673F	31
F3	1673F	C908Y	31
F4	R193W	Splice (1244+2T→G)	31
F5	Splice (686+1G→A)	R1123C	31

is one of the quality-control mechanisms that ensure high fidelity of gene expression. The NMD pathway destroys aberrant mRNAs that contain premature termination codons.[32,33] Therefore, ADAMTS-13 mutants with nonsense mutations may not be translated in vivo.

Frameshift Mutations

Five frameshift mutations have been identified: 1783delTT, 2376del26 (2376-2401del), 2549delAT, 3769insT, and 4143insA. If these mutated forms of ADAMTS-13 were to be translated, truncated mutants with aberrant C-terminal ends would be expressed. Each mutation replaces L595-T1427 with GGEDRRALCRGWEDEHLP, A793-T1427 with PALPCQVGGVRAQLMHISWWSRPGLGERDLCARGRWPGGSSD, D850-T1427 with GEAACP, L1258-T1427 with VGHDFQLQDQHAGGEAALRAARRWGAAAVWEPACS, or E1382-T1427 with REQPG, respectively. Some of these forms may not be secreted, and others may be secreted but dysfunctional. However, like the nonsense mutations described above, mRNAs with these frameshift mutations might be eliminated by gene expression quality-control systems.

Splice Mutations

Four splice mutations have been found: 414+1G→A, 686+1G→A, 1244+2T→G, and 1584+5G→A. The 414+1G→A (intron 4), 686+1G→A (intron 6), and 1244+2T→G (intron 10) mutations cause inconsistencies with the GT-AG rules of mRNA splicing. The 1584+5G→A (intron 13) mutation also alters the donor splice site from the consensus sequence. In fact, the effect of each of these mutations on mRNA splicing was examined experimentally. Total RNAs were isolated from patients' lymphoblasts or whole blood cells and used as templates for reverse-transcriptase polymerase chain reaction (RT-PCR). The data indicated that little or no normally spliced products were generated from the mutant alleles.[19,31]

Frequency of TTP-Causing Mutations

All 33 mutations were excluded as common sequence polymorphisms by screening a large panel of unaffected chromosomes. However, nine of these mutations occur on several occasions in 23 TTP patients (Table 2). Notably, this multiplicity occurs within the subjects of each investigator group. This suggests that *ADAMTS13* mutations may be specific to limited areas rather than be shared across the world. Specifically, Schneppenheim et al identified four alleles with the frameshift mutation 4143insA in seven unrelated German patients,[28] suggesting that the mutation is a relatively common polymorphism in areas as compared with other rare mutations.

Although most patients with hereditary TTP are compound heterozygotes at the *ADAMTS13* gene, some patients are homozygotes. Levy et al identified three patients with homozygous R692C mutations,

Table 3. Common Missense SNPs Identified in the *ADAMTS13* Gene

Exon	Nucleotide	AA	Domain	References
1	19C→T	R7W	Signal peptide	19,29
12	1342C→G	Q448E	Cysteine-rich	19,27,29
12	1423C→T	P475S	Cysteine-rich	27
16	1852C→G	P618A	Spacer	19,29
16	1874G→A	R625H	Spacer	19
18	2195C→T	A732V	Tsp1-2	19,29
21	2699C→T	A900V	Tsp1-5	19
24	3097G→A	A1033T	Tsp1-7	19

who all came from the same small village where the families lived for several generations.[19] We identified a homozygous patient with a Q449X mutation, whose two great-grandparents came from the same village in the northeastern region of the Japanese mainland at the end of the 19th century.[27] The patient with the homozygous 414+1G→A splice mutation had a family history of consanguineous marriage.[31] The patient with the homozygous L232Q mutation also likely came from a consanguineous pedigree, based on analysis of an intragenic haplotype.[28] The patient with the homozygous 1783delTT frameshift mutation was born to parents who were first cousins of Yemenite background.[30] Thus, all five homozygous mutations appear to be the progeny of some blood relationship.

Common Single-Nucleotide Polymorphisms

In all, eight missense mutations were reported as common single-nucleotide polymorphisms (SNPs)[19,27,29] (Table 3). In addition, Levy et al reported eight silent SNPs in eight exons and 10 SNPs in eight introns.[19] Thus far, no relationship between these SNPs and the development of TTP has been suspected.

The allele frequencies of R7W, Q448E, P475S, and P618A SNPs have been reported. We sequenced 364 Japanese subjects without TTP, and identified 125 heterozygotes and eight homozygotes of Q448E, and 35 heterozygotes and one homozygote of P475S. The allele frequencies were calculated to be 19% and 5%, respectively.[27] Since a 43% frequency of Q448E was also determined among 120 European alleles,[29] this SNP seems to be spread worldwide. In contrast, the P475S SNP was only reported by us. We sequenced 95 Caucasian subjects and found no alleles positive for the SNP (unpublished data, January 2003). Therefore, the P475S SNP may be localized to restricted areas around Japan. Antoine et al also reported the allele frequencies of R7W and P618A, as 10% and 9%, respectively.[29]

We prepared recombinant ADAMTS-13 with Q448E or P475S mutations and measured their cleavage activities toward VWF multimers.[27] The Q448E mutant showed normal activity, whereas the P475S mutant had a significantly reduced activity (~5% to 10% of wild type). The allele frequency of P475S is about 5%, as described above, suggesting that approximately 10% of the Japanese population are heterozygotes and may possess significantly reduced ADAMTS-13 activity. Theoretically, one in 400 Japanese may be P475S homozygotes, with quite low activity.

Sequencing Methods

We have performed *ADAMTS13* sequence analysis as described previously[27] with a slight modification. This analysis was carried out with the permission of ethics committees. Human genomic DNA was isolated from whole blood using the FlexiGene DNA kit (Qiagen, Hilden, Germany) or an automated nucleic acid isolation system, NA-3000 (Kurabo, Osaka, Japan). All exons of the *ADAMTS13* gene, including the intron-exon boundaries, were PCR-amplified with corresponding intronic primers (Table 4). Twenty-six primer sets were used. PCR was performed using HotStarTaq DNA polymerase (Qiagen) or the GC-RICH PCR system (Roche, Tokyo, Japan). For all exons, except 7 and 8, 10 μL of HotStarTaq Master Mix was added to 10 μL of water containing 50 ng of genomic DNA, 1 μmol/L forward primer, and 1 μmol/L reverse primer. For the amplification of exon 7, 0.4 μL of GC-RICH Enzyme Mix was added to 19.6 μL of water containing 50 ng of genomic DNA, 0.25 μmol/L forward primer, 0.25 μmol/L reverse primer, 0.2 mmol/L dNTP, and 4 μL of 5× GC-RICH PCR reaction buffer. For exon 8, 10 μL of HotStarTaq Master Mix was added to 10 μL of water containing 250 ng of genomic DNA, 4 μmol/L forward primer, 4 μmol/L reverse primer, and 5% dimethyl sulfoxide. The thermal cycle conditions for each reaction are summarized in Table 4. PCR products were purified using the QIAquick PCR Purification kit (Qiagen), and sequenced in both directions using a BigDye Terminator Kit (Applied Biosystems, Foster City, CA) and a 3700 DNA Analyzer (Applied Biosystems).

Future Issues

The coming sequence analysis of hereditary TTP patients will likely reveal still more *ADAMTS13* mutations. At present, it is difficult to define a correlation between each genotype and phenotype for TTP patients. Patients with hereditary TTP differ greatly in the age of onset and severity of symptoms. About half of hereditary TTP patients have their first acute episode during childhood, while the other half are

Table 4. Amplification of *ADAMTS13* Exons

Exon (bp)	Forward Primer	Reverse Primer	Product (bp)	PCR Step 1	PCR Step 2
1 (549)	GATTGCCAGGCCGTTTGTGAT	GCAAACCCCAAAGCTGATGTA	768	95°C/15 min	(94°C/20 s, 63°C/20 s, 72°C/45 s) × 40
2 (67)	CCTCGGTCTCCCCAAGTGTTA	GAACCCTGGCCTGGCTGGAAC	348	95°C/15 min	(94°C/20 s, 60°C/20 s, 72°C/45 s) × 35
3 (158)	GGTGGGGGTGACACGCAATGT	CCAGGGGAGGGAGGGAGAAGA	437	95°C/15 min	(94°C/20 s, 60°C/20 s, 72°C/45 s) × 35
4 (84)	TGTTTTCCTTGCGTTAGTTGG	GAGGATGGAGATGCGATGACT	382	95°C/15 min	(94°C/20 s, 60°C/20 s, 72°C/45 s) × 35
5-6 (125, 147)	AACAAACCGACCGCAGTCAGC	GGTTCCCCTGTCCTCACACCT	638	95°C/15 min	(94°C/20 s, 60°C/20 s, 72°C/45 s) × 35
7 (138)	GCTGGCGCTGCGGCACTAGGG	GTTGGACGGAGGGGTGGGTTG	399	95°C/3 min	(95°C/30 s, 64°C/30 s, 72°C/45 s) × 38
8 (163)	ACTCCTCCGTCCCGCCTCCTC	GCCCTCCCAGGACTAGCTACA	477	95°C/15 min	(94°C/20 s, 64°C/20 s, 72°C/30 s) × 40
9 (105)	GTGCAGAGTGTTGGCTGTGTC	CTCTGCCCCATACTGGTCCTG	334	95°C/15 min	(94°C/20 s, 60°C/20 s, 72°C/45 s) × 35
10-11 (152, 64)	TGAGGATGTTGGGGGACTCTC	CAAATGTGTCCTGGTGTGAAC	512	95°C/15 min	(94°C/20 s, 60°C/20 s, 72°C/45 s) × 35
12 (127)	TGAGGCCACACCCACATCTTG	ATGCCAGAGCCTGAACCACTT	366	95°C/15 min	(94°C/20 s, 60°C/20 s, 72°C/45 s) × 35
13 (149)	ATAGAAACCCTTGCCCCAGAT	ATCCTTTTCCCCAGCACCACT	390	95°C/15 min	(94°C/20 s, 63°C/20 s, 72°C/45 s) × 40
14 (121)	CAGGGCTGCAGAGTCATTGAG	GAAGGGTGGCGAAGTGGAAGA	358	95°C/15 min	(94°C/20 s, 60°C/20 s, 72°C/45 s) × 35
15 (81)	CTCCCTTTGTCTGTGGTGTGG	ACTATCAAGCCTGAGGGTGGT	279	95°C/15 min	(94°C/20 s, 60°C/20 s, 72°C/45 s) × 35
16 (182)	GGGACCCCGGGAAGGAGAGTC	GTAAGTGACCGCTGAATGAAT	393	95°C/15 min	(94°C/20 s, 60°C/20 s, 72°C/45 s) × 35
17-18 (136, 130)	GGCCAGGCTGGAGTGCTATGT	CAGAATGGGGGCACTCACAGA	770	95°C/15 min	(94°C/20 s, 63°C/20 s, 72°C/45 s) × 40
19 (186)	ACCAGCCTGTGATTCGGTTGT	AGGAACTCTGACAGCAGCACT	548	95°C/15 min	(94°C/20 s, 60°C/20 s, 72°C/45 s) × 35
20 (190)	CTCTTTGGGCTCCTGGATGTT	CAATGGGTGCTCCTCGTTCTC	386	95°C/15 min	(94°C/20 s, 60°C/20 s, 72°C/45 s) × 35
21 (121)	AAGGATACCCGCTGCGAGACC	AGCCAATCAACACCCACATTT	489	95°C/15 min	(94°C/20 s, 60°C/20 s, 72°C/45 s) × 35
22 (130)	CCATGCGGGCCTTATGTGCTA	TCTGGGTTGCAGTCCTCAAAG	439	95°C/15 min	(94°C/20 s, 60°C/20 s, 72°C/45 s) × 35
23 (183)	GGGGGCCTCCAGAAAGAGAAC	GTGTTGCCCAGGTTGGACTTG	476	95°C/15 min	(94°C/20 s, 60°C/20 s, 72°C/45 s) × 35
24 (205)	GGCTCAGTGGCTGCACTTTCC	TCCAGCGTCCCCAAACCTAAG	576	95°C/15 min	(94°C/20 s, 60°C/20 s, 72°C/45 s) × 35
25 (319)	GACAGGGACCCAGACTTGAAT	AAGTTACTTCCCCTTGATAGT	729	95°C/15 min	(94°C/20 s, 60°C/20 s, 72°C/45 s) × 35
26 (147)	CTGCATGTGCCCCCTCTTGCT	TGGGCACATCACTTAATCTCT	574	95°C/15 min	(94°C/20 s, 60°C/20 s, 72°C/45 s) × 35
27 (177)	GTGCATTCCCACCTGTAGTTT	TCCCTGGCACGTGCAGACTGA	583	95°C/15 min	(94°C/20 s, 60°C/20 s, 72°C/45 s) × 35
28 (185)	CCAGAGCCCAGAACATTTAGC	GCCACTATTTCACTCTTGTAG	581	95°C/15 min	(94°C/20 s, 60°C/20 s, 72°C/45 s) × 35
29 (412)	GTGTCCTTGGGGAAGTGATGT	GATTGGATTTTCTTCCTGGAT	757	95°C/15 min	(94°C/20 s, 60°C/20 s, 72°C/45 s) × 35

NOTE. All exons except exon 7 are amplified using HotStarTaq DNA polymerase. Exon 7 is amplified using GC-RICH PCR system. The reaction mixture for exon 8 contains 5% dimethyl sulfoxide.

affected in adulthood. Symptoms in adults often develop in association with stress of infection or pregnancy.[34] Genetic backgrounds other than *ADAMTS13* or environmental factors may be associated with the etiology of TTP.

From the viewpoint of clinical genetics, some problems still remain to be resolved. First, is the genetic variation in *ADAMTS13*, including common SNPs, associated with acquired TTP? Although the majority of TTP is the acquired type, with autoantibodies to ADAMTS-13, almost all subjects analyzed so far have had hereditary TTP. Sequence analysis of many patients with acquired TTP may help answer this question.

Second, are common SNPs that influence VWF-cleaving activity associated with other diseases? Although the almost complete loss of ADAMTS-13 activity results in TTP, the decreased activity may also be a risk factor for some thrombotic diseases, due to large circulating VWF multimers. In fact, a recent report suggested that levels of ADAMTS-13 activity are decreased in patients with coronary heart disease.[35] Common SNPs causing less than normal activity may also be linked to other disorders. The epidemiologic assessment of the P475S SNP will be important, at least in Japan.

Third, can VWF mutation be responsible for TTP? All hereditary TTP patients analyzed so far had mutations in *ADAMTS13*, and no *VWF* mutations were identified. Many mutations of *VWF* that enhance susceptibility to ADAMTS-13 and lead to the loss of large VWF multimers have been identified as the cause of type 2A von Willebrand disease. In contrast, no mutations conferring resistance against ADAMTS-13 proteolysis have been found. Such mutations might be lethal in the uterus. Analysis of genetically engineered animals may be useful to investigate this issue.

Fourth, do mutations causing deficiency of *THBS1*, which encodes thrombospondin-1, cause TTP? Two molecules are known that control the size of VWF multimers, ADAMTS-13 and thrombospondin-1. The latter is a trimeric glycoprotein that uncouples VWF multimers by reducing the disulfide-bonds that link individual subunits.[36,37] A combination of common genetic variations of *ADAMTS13*, *VWF*, and *THBS1* may be associated with TTP and other thrombotic diseases.

Additional Information

At the same time as the deadline for this manuscript, the 19th Congress of the International Society on Thrombosis and Haemostasis was held in Birmingham, UK. Eighteen additional mutations causing TTP were reported there by three research groups.[38-40] Reduced activity of some mutants was confirmed by expression analysis. The activities of recombinant ADAMTS-13 with common SNPs, R7W, P618A, A900V, and A1033T, were also measured.[41] The P475S SNP was also found in the Chinese population, but its allele frequency was remarkably lower than that in the Japanese population.[42]

References

1. Moschcowitz E: Hyaline thombrosis of the terminal arterioles and capillaries; a hitherto undescribed disease. Proc NY Pathol Soc 24:21-24, 1924
2. Kinoshita S, Yoshioka A, Park YD, Ishizashi H, Konno M, Funato M, et al: Upshaw-Schulman syndrome revisited: A concept of congenital thrombotic thrombocytopenic purpura. Int J Hematol 74:101-108, 2001
3. Fujimura Y, Titani K: Structure and function of von Willebrand factor, in Bloom AL, Forbes CD, Thomas DP, Tuddenham EGD (eds): Haemostasis and Thrombosis. New York, NY, Churchill Livingstone, 1994, pp 379-395
4. Furlan M: Von Willebrand factor: Molecular size and functional activity. Ann Hematol 72:341-348, 1996
5. Ruggeri ZM: von Willebrand factor. J Clin Invest 99:559-564, 1997
6. Sadler JE: Biochemistry and genetics of von Willebrand factor. Annu Rev Biochem 67:395-424, 1998
7. Chung DW, Fujikawa K: Processing of von Willebrand factor by ADAMTS-13. Biochemistry 41:11065-11070, 2002
8. Fujimura Y, Matsumoto M, Yagi H, Yoshioka A, Matsui T, Titani K: Von Willebrand factor-cleaving protease and Upshaw-Schulman syndrome. Int J Hematol 75:25-34, 2002
9. George JN, Sadler JE, Lämmle B: Platelets: Thrombotic thrombocytopenic purpura. Hematology (Am Soc Hematol Educ Program) 9:315-334, 2002
10. Zheng X, Majerus EM, Sadler JE: ADAMTS13 and TTP. Curr Opin Hematol 9:389-394, 2002
11. Tsai HM: Platelet activation and the formation of the platelet plug: Deficiency of ADAMTS13 causes thrombotic thrombocytopenic purpura. Arterioscler Thromb Vasc Biol 23:388-396, 2003
12. Furlan M, Robles R, Galbusera M, Remuzzi G, Kyrle PA, Brenner B, et al: von Willebrand factor-cleaving protease in thrombotic thrombocytopenic purpura and the hemolytic-uremic syndrome. N Engl J Med 339:1578-1584, 1998
13. Tsai HM, Lian EC: Antibodies to von Willebrand factor-cleaving protease in acute thrombotic thrombocytopenic purpura. N Engl J Med 339:1585-1594, 1998
14. Fujikawa K, Suzuki H, McMullen B, Chung D: Purification of human von Willebrand factor-cleaving protease and its identification as a new member of the metalloproteinase family. Blood 98:1662-1666, 2001
15. Gerritsen HE, Robles R, Lämmle B, Furlan M: Partial amino acid sequence of purified von Willebrand factor-cleaving protease. Blood 98:1654-1661, 2001
16. Soejima K, Mimura N, Hirashima M, Maeda H, Hamamoto T, Nakagaki T, et al: A novel human metalloprotease synthesized in the liver and secreted into the blood: Possibly, the von Willebrand factor-cleaving protease? J Biochem 130:475-480, 2001
17. Zheng X, Chung D, Takayama TK, Majerus EM, Sadler JE, Fujikawa K: Structure of von Willebrand factor-cleaving protease (ADAMTS13), a metalloprotease involved in thrombotic thrombocytopenic purpura. J Biol Chem 276:41059-41063, 2001

18. Plaimauer B, Zimmermann K, Volkel D, Antoine G, Kerschbaumer R, Jenab P, et al: Cloning, expression, and functional characterization of the von Willebrand factor-cleaving protease (ADAMTS13). Blood 100:3626-3632, 2002
19. Levy GG, Nichols WC, Lian EC, Foroud T, McClintick JN, McGee BM, et al: Mutations in a member of the ADAMTS gene family cause thrombotic thrombocytopenic purpura. Nature 413:488-494, 2001
20. Cal S, Obaya AJ, Llamazares M, Garabaya C, Quesada V, López-Otín C: Cloning, expression analysis, and structural characterization of seven novel human ADAMTSs, a family of metalloproteinases with disintegrin and thrombospondin-1 domains. Gene 283:49-62, 2002
21. Dent JA, Berkowitz SD, Ware J, Kasper CK, Ruggeri ZM: Identification of a cleavage site directing the immunochemical detection of molecular abnormalities in type IIA von Willebrand factor. Proc Natl Acad Sci USA 87:6306-6310, 1990
22. Tsai HM, Sussman II, Nagel RL: Shear stress enhances the proteolysis of von Willebrand factor in normal plasma. Blood 83:2171-2179, 1994
23. Furlan M, Robles R, Lämmle B: Partial purification and characterization of a protease from human plasma cleaving von Willebrand factor to fragments produced by in vivo proteolysis. Blood 87:4223-4234, 1996
24. Tsai HM: Physiologic cleavage of von Willebrand factor by a plasma protease is dependent on its conformation and requires calcium ion. Blood 87:4235-4244, 1996
25. Zheng X, Nishio K, Majerus EM, Sadler JE: Cleavage of von Willebrand factor requires the spacer domain of the metalloprotease ADAMTS13. J Biol Chem 278:30136-30141, 2003
26. Soejima K, Matsumoto M, Kokame K, Yagi H, Ishizashi H, Maeda H, et al: ADAMTS-13 cysteine-rich/spacer domains are functionally essential for von Willebrand factor cleavage. Blood 102:3232-3237, 2003
27. Kokame K, Matsumoto M, Soejima K, Yagi H, Ishizashi H, Funato M, et al: Mutations and common polymorphisms in ADAMTS13 gene responsible for von Willebrand factor-cleaving protease activity. Proc Natl Acad Sci USA 99:11902-11907, 2002
28. Schneppenheim R, Budde U, Oyen F, Angerhaus D, Aumann V, Drewke E, et al: von Willebrand factor cleaving protease and ADAMTS13 mutations in childhood TTP. Blood 101: 1845-1850, 2003
29. Antoine G, Zimmermann K, Plaimauer B, Grillowitzer M, Studt JD, Lämmle B, et al: ADAMTS13 gene defects in two brothers with constitutional thrombotic thrombocytopenic purpura and normalization of von Willebrand factor-cleaving protease activity by recombinant human ADAMTS13. Br J Haematol 120:821-824, 2003
30. Savasan S, Lee SK, Ginsburg D, Tsai HM: ADAMTS13 gene mutation in congenital thrombotic thrombocytopenic purpura with previously reported normal VWF cleaving protease activity. Blood 101:4449-4451, 2003
31. Matsumoto M, Kokame K, Soejima K, Miura M, Hayashi S, Fujii Y, et al: Molecular characterization of ADAMTS13 gene mutations in Japanese patients with Upshaw-Schulman syndrome. Blood (in press)
32. Wagner E, Lykke-Andersen J: mRNA surveillance: the perfect persist. J Cell Sci 115:3033-3038, 2002
33. Wilkinson MF, Shyu AB: RNA surveillance by nuclear scanning? Nat Cell Biol 4:E144-147, 2002
34. Furlan M, Lämmle B: Aetiology and pathogenesis of thrombotic thrombocytopenic purpura and haemolytic uraemic syndrome: The role of von Willebrand factor-cleaving protease. Best Pract Res Clin Haematol 14:437-454, 2001
35. Yoo G, Blomback M, Schenck-Gustafsson K, He S: Decreased levels of von Willebrand factor-cleaving protease in coronary heart disease and thrombotic thrombocytopenic purpura: Study of a simplified method for assaying the enzyme activity based on ristocetin-induced platelet aggregation. Br J Haematol 121:123-129, 2003
36. Xie L, Chesterman CN, Hogg PJ: Control of von Willebrand factor multimer size by thrombospondin-1. J Exp Med 193: 1341-1349, 2001
37. Pimanda JE, Annis DS, Raftery M, Mosher DF, Chesterman CN, Hogg PJ: The von Willebrand factor-reducing activity of thrombospondin-1 is located in the calcium-binding/C-terminal sequence and requires a free thiol at position 974. Blood 100:2832-2838, 2002
38. Motto D, Levy G, Mcgee B, Tsai H, Ginsburg D: ADAMTS13 mutations identified in familial TTP patients result in loss of VWF-cleaving protease activity. J Thromb Haemost 1:OC115, 2003 (suppl 1)
39. Schneppenheim R, Angerhaus D, Mainusch K, Obser T, Oyen F, Budde U: Comparative expression of recombinant wild-type and mutant von Willebrand factor cleaving protease ADAMTS13. J Thromb Haemost 1:OC117, 2003 (suppl 1)
40. Veyradier A, Lavergne JM, Obert B, Ribba AS, Fressinaud E, Loirat C, et al: Identification of seven new candidate mutations of ADAMTS13 gene in four French families related to congenital thrombotic thrombocytopenic purpura. J Thromb Haemost 1:P0310, 2003 (suppl 1)
41. Peyvandi F, Lavoretano S, Canciani MT, Mannucci PM: In vitro expression study of four single nucleotide polymorphisms in the ADAMTS13 gene. J Thromb Haemost 1:P0325, 2003 (suppl 1)
42. Gao WQ, Wang ZY, Bai X, Ruan C: The frequency of P475S polymorphism in von Willebrand factor-cleaving protease among Chinese population and its relevance to arterial thrombotic disorders. J Thromb Haemost 1:P0376, 2003 (suppl 1)

THE JOURNAL OF BIOLOGICAL CHEMISTRY
Vol. 279, No. 29, Issue of July 16, pp. 30896–30903, 2004
Printed in U.S.A.

Identification of Strain-specific Variants of Mouse *Adamts13* Gene Encoding von Willebrand Factor-cleaving Protease*

Received for publication, December 26, 2003, and in revised form, May 7, 2004
Published, JBC Papers in Press, May 10, 2004, DOI 10.1074/jbc.M314184200

Fumiaki Banno‡, Kazuyoshi Kaminaka§, Kenji Soejima§, Koichi Kokame‡, and Toshiyuki Miyata‡¶

From the ‡National Cardiovascular Center Research Institute, Osaka 565-8565, Japan and the §First Research Department, The Chemo-Sero-Therapeutic Research Institute, Kumamoto 869-1298, Japan

Human *ADAMTS13* was recently identified as a gene encoding von Willebrand factor-cleaving protease, hADAMTS13. Both congenital and acquired defects in this enzyme can cause thrombotic thrombocytopenic purpura. hADAMTS13 consists of 1,427 amino acid residues and is composed of multiple structural domains including thrombospondin type 1 motifs and CUB domains. To analyze the functional roles of these domains *in vivo*, we determined the cDNA sequence of the mouse ortholog, mADAMTS13. Unexpectedly, two forms of the mouse *Adamts13* gene were isolated that differed in the insertion of an intracisternal A particle (IAP) retrotransposon including a premature stop codon. The IAP insertion was found in BALB/c, C3H/He, C57BL/6, and DBA/2 strains but not in the 129/Sv strain. The outbred ICR strain had either the IAP-free or IAP-inserted allele or both. IAP-free *Adamts13* encoded mADAMTS13L, a protein of 1,426 amino acid residues with the same domain organization as hADAMTS13. In contrast, IAP-inserted *Adamts13* encoded a C-terminally truncated enzyme, mADAMTS13S, that is comprised of only 1,037 amino acid residues and lacking the C-terminal two thrombospondin type 1 motifs and two CUB domains. Strain specificity was also confirmed by reverse transcription-PCR and Northern blot analyses. Both recombinant mADAMTS13L and mADAMTS13S exhibited von Willebrand factor cleaving activities *in vitro*. The natural variation in mouse ADAMTS13 should allow for the determination of hitherto unknown functions of its C-terminal domains *in vivo*.

von Willebrand factor (VWF)[1] is a large glycoprotein that mediates adhesion between the platelet surface and damaged subendothelium (1, 2). VWF is mainly synthesized in endothelial cells and secreted into the circulating blood as unusually large VWF (UL-VWF) multimers (1, 2). In healthy individuals, UL-VWF multimers are cleaved to smaller sizes in plasma (3). If cleavage is impaired, however, UL-VWF multimers accumulate in the plasma. Because UL-VWF multimers possess an extremely high thrombotic activity (4, 5), UL-VWF multimers in the circulation lead to platelet clumping at the sites of vascular injury. The importance of VWF proteolysis is best illustrated by the severe consequences of thrombotic thrombocytopenic purpura, a condition associated with increased levels of UL-VWF multimers (6). This disease is characterized by microangiopathic hemolytic anemia, thrombocytopenia, neurological dysfunction, renal failure, and fever (7). The mortality of affected patients may exceed 90% without treatment such as plasma exchange.

Human ADAMTS13 (hADAMTS13), an enzyme responsible for the proteolytic processing of UL-VWF multimers, was recently purified, and its partial amino acid sequence was determined (8–10). hADAMTS13 cleaves a peptidyl bond between Tyr^{1605} and Met^{1606} in the VWF A2 domain (11–13). The gene encoding hADAMTS13 was identified as a member of the "a disintegrin-like and metalloprotease with thrombospondin type 1 motif (ADAMTS)" family and designated as *ADAMTS13* (8, 14, 15). *ADAMTS13* contains 29 exons and spans ~37 kb on chromosome 9q34 (8, 14, 15). The mRNA is detected primarily in liver (8, 14, 15). Analysis of genomic DNA in patients with congenital thrombotic thrombocytopenic purpura revealed that mutations of *ADAMTS13* could lead to an inactive enzyme (15–20). Notably, a common single nucleotide polymorphism, P475S, with ~10% heterozygosity in the Japanese population, resulted in a decrease of enzymatic activity (16).

hADAMTS13 consists of several different domains: a signal peptide, a propeptide, a reprolysin-like metalloprotease domain, a disintegrin-like domain, a thrombospondin type 1 (TSP1) motif, a cysteine-rich domain, a spacer domain, seven additional TSP1 repeats, and two CUB domains. *In vitro* studies using C-terminally truncated hADAMTS13 constructs revealed that the C-terminal TSP1 motifs and CUB domains were dispensable to maintain the VWF cleaving activity (21, 22). However, the biochemical and physiological roles of these domains *in vivo* remain to be resolved. As a first step to develop suitable animal models for following potential roles of this enzyme *in vivo*, we have cloned the mouse ortholog of hADAMTS13, mADAMTS13, and determined its complete genomic structure. In the present study, we report two types of the *Adamts13* gene in mice caused by the strain-specific insertion of an intracisternal A-particle (IAP) retrotransposon. We further examine the VWF cleaving activity of mADAMTS13.

* This work was supported in part by grants-in-aid from the Ministry of Health, Labor, and Welfare of Japan; from the Ministry of Education, Culture, Sports, Science, and Technology of Japan; from the Japan Society for the Promotion of Science; and from the Program for Promotion of Fundamental Studies in Health Sciences of the Organization for Pharmaceutical Safety and Research of Japan. The costs of publication of this article were defrayed in part by the payment of page charges. This article must therefore be hereby marked "*advertisement*" in accordance with 18 U.S.C. Section 1734 solely to indicate this fact.

The nucleotide sequence(s) reported in this paper has been submitted to the DDBJ/GenBank™/EBI Data Bank with accession number(s) AB071302, AB095445, and AB112362.

¶ To whom correspondence should be addressed: National Cardiovascular Center Research Institute, 5-7-1 Fujishirodai, Suita, Osaka 565-8565, Japan. Tel.: 81-6-6833-5012; Fax: 81-6-6835-1176; E-mail: miyata@ri.ncvc.go.jp.

[1] The abbreviations used are: VWF, von Willebrand factor; TSP1, thrombospondin type 1; UL-VWF, unusually large VWF; IAP, intracisternal A-particle; GST, glutathione *S*-transferase; RACE, rapid amplification of cDNA ends; RT, reverse transcription; ORF, open reading frame; h, human; m, mouse; HRP, horseradish peroxidase.

EXPERIMENTAL PROCEDURES

Animals—Male 129/Sv mice were purchased from Clea Japan, Inc. Male BALB/c, C3H/He, C57BL/6, DBA/2, and ICR mice were purchased from Japan SLC, Inc. Blood (~100 μl) was collected by cardiac puncture into a syringe containing 10 μl of 3.8% sodium citrate and centrifuged to obtain plasma. Spleen and liver were excised, rinsed in phosphate-buffered saline, and immediately used for DNA and RNA preparation.

DNA Sequencing—All of the sequence analyses were performed by 373A or 3700 automated DNA sequencer (Applied Biosystems) with a BigDye Terminator Kit (Applied Biosystems).

Determination of the mADAMTS13 cDNA Sequence—Total RNA was prepared from the livers of C57BL/6 and 129/Sv mice with Isogen (Nippon Gene), and poly(A)$^+$ RNA was purified with an mRNA purification kit (Amersham Biosciences) according to the manufacturer's instruction. The cDNA was synthesized from the poly(A)$^+$ RNA with a first strand cDNA synthesis kit (Amersham Biosciences). PCR was carried out with primers designed from the genomic DNA sequence (forward sequence in 5′-untranslated region, 5′-AGGAAGCTCCCAAG-AGTAAACACTGCCT-3′; reverse sequence within the metalloprotease domain, 5′-TCAGAGAGGGTGATTAGCTTCACCAGGT-3′). PCR products were cloned into pCR2.1 vector using a TA Cloning™ kit (Invitrogen) and sequenced.

In addition, 3′-RACE was performed using a 3′-Full RACE Core Set (Takara), according to the manufacturer's instructions. After reverse transcription from liver poly(A)$^+$ RNA, PCR was performed using the Adaptor Primer provided with the kit and a gene-specific forward primer within the metalloprotease domain, 5′-TGGAGTTGCCTGATG-GCAACCAGCA-3′. The second PCR was performed using the first PCR products as a template with Adaptor Primer and a gene-specific internal forward primer, 5′-CATCACCTTTTCCTACTTTCAACTGAAGC-AG-3′. The cycling parameters were as follows: 35 cycles of 94 °C for 30 s, 55 °C for 30 s, and 72 °C for 3 min, followed by 72 °C for 7 min. PCR products were cloned into pCR2.1 vector and sequenced.

PCR Analysis of IAP Insertion in the Adamts13 Gene—Genomic DNA was extracted from ear punches of 129/Sv, BALB/c, C3H/He, C57BL/6, DBA/2, and ICR mice by DNeasy Tissue Kit (Qiagen). Presence or absence of an IAP insertion in the *Adamts13* gene was determined by PCR with HotStarTaq DNA polymerase (Qiagen). The amplification was carried out using mixture of three primers; the intron 23-specific forward primer, 5′-ACCTCTCAAGTGTTTGGGATGCTA-3′, the IAP-specific reverse primer, 5′-TCAGCGCCATCTTGTGACGGCGAA-3′, and the primer downstream of the IAP target site, 5′-TGCCAGATGG-CCATGATTAACTCT-3′. PCR products were directly sequenced.

Southern Blot Analysis—Genomic DNA prepared from spleens was digested with EcoRV, separated on 0.7% agarose gel, and transferred to a nylon membrane by standard capillary blotting techniques. A genomic fragment (842 bp) upstream of the IAP target site was produced by PCR with the primers 5′-TAGGCAGCCATGGATCTGTATTAG-3′ and 5′-TGTCTGCTCTTCCAGAAATCCTTA-3′ and labeled with fluorescein-11-dUTP using Gene Images random prime labeling module (Amersham Biosciences). The blot was hybridized with the probe, and the hybridized probe was detected using the Antifluorescein-AP conjugate and the CDP-*Star* detection reagent (Amersham Biosciences) according to the manufacturer's instructions. Chemiluminescence was measured by an LAS-1000plus image analyzer (Fujifilm).

Determination of the Adamts13 Genomic Sequence—A λ phage library constructed from Sau3AI-digested genomic DNA of the 129/Sv strain was screened by a PCR-based method as described previously (23). Three independent positive phages were obtained. Each phage insert DNA was subcloned into pBluescript II SK(+) vector (Stratagene) and sequenced using the GPS-1 Genome Priming System (New England Biolabs) according to the manufacturer's instructions. The sequence data were assembled and analyzed using the Sequencher software (Gene Codes). Sequence gaps of each target DNA were filled by primer walking sequencing.

Reverse Transcription-PCR—Total RNA was extracted from the livers of six mouse strains with Isogen (Nippon Gene), and poly(A)$^+$ RNA was purified using PolyATtract mRNA Isolation Systems (Promega) and subjected to one-step RT-PCR (Qiagen). The exon 21/22-specific sense primer (5′-TTGTGGGAGAGGTCTGAAGGAACT-3′), the pseudo-exon 24-specific antisense primer (5′-TCAGCGCCATCTTGTGACGGC-GAA-3′), and the exon 24/25-specific antisense primer (5′-ACAGGAG-ACAGAGCACTCTGTCCA-3′) were simultaneously used for the amplification. The PCR products were excised from the agarose gel and sequenced.

Northern Blot Analysis—The specific fluorescein-labeled probe (1.3 kb) was synthesized by PCR from mouse *Adamts13* cDNA as described previously (23). The primers used were a sense primer located in exon 3 (5′-ATTCTGCACCTGGAACTCCTGGTA-3′) and an antisense primer located in exon 13 (5′-CGGCTGACAATGAAGCTTTCTCCA-3′). Poly(A)$^+$ RNA (10 μg) from mouse livers were separated on 1% agarose gel containing 2% formaldehyde and transferred to a nylon membrane. Hybridization and detection using the Antifluorescein-AP conjugate and the CDP-*Star* detection reagent (Amersham Biosciences) were performed according to the manufacturer's instructions. Commercially available premade Northern blot membranes containing poly(A)$^+$ RNA from the BALB/c strain (Multiple Tissue Northern blot; Clontech) and the Swiss Webster strain (FirstChoice Northern blot; Ambion) were also analyzed using the Antifluorescein-HRP conjugate and the DNA Thunder Chemiluminescence Reagent Plus (PerkinElmer Life Sciences). Chemiluminescence was measured by an LAS-1000plus image analyzer (Fujifilm).

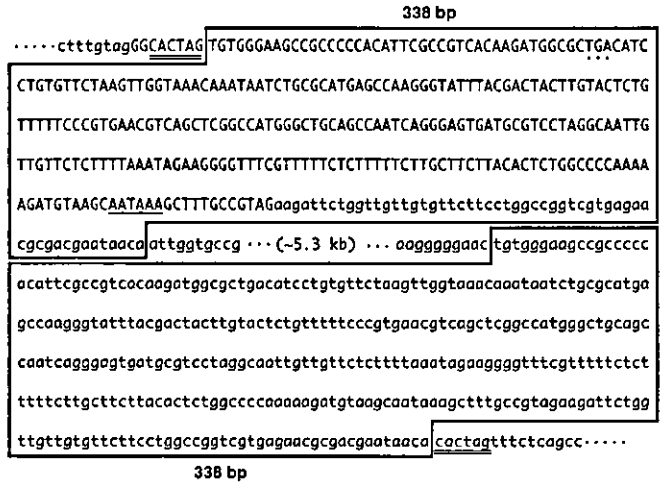

FIG. 1. **Nucleotide sequence of the retrovirus-like element observed in *Adamts13* intron 23 of the C57BL/6 strain.** The 338-bp repetitive sequences of a retrovirus-like element are *boxed*. The 6-bp duplication of target DNA at the insertion site is *double underlined*. Exon 24 of the C57BL/6 strain, shown in *uppercase letters*, contains a stop codon TGA (*dotted*) and a putative polyadenylation signal AATAAA (*underlined*).

Preparation of Recombinant Substrate (mVWF73) for Enzymatic Assay—To examine the enzymatic activities of mADAMTS13, we prepared the recombinant substrate as described previously (24). In brief, a D1596-T1668 region of mouse VWF was amplified by RT-PCR using total RNA from a C57BL/6 mouse liver. The primers, 5′-cgggatccGAC-CGGGTAGAGGCACCTAACC-3′ and 5′-cggaattcTCAGTGATGGTGA-TGGTGATGTGTCTCGCAGGACCAGGTCAGGA-3′ were used for the amplification. Lowercase letters indicate added restriction enzyme sites, and the underlined sequence is the inserted C-terminal His_6 tag (H). The PCR product was digested with BamHI and EcoRI and cloned into the corresponding sites of pGEX-6P-1 (Amersham Biosciences), a glutathione S-transferase (GST) fusion expression vector. The resulting plasmid encoding GST-D1596T1668-H was introduced into *Escherichia coli*, BL21 (Stratagene), and expression was induced by the addition of isopropyl-β-D-thiogalactoside. The bacterial cells were collected and lysed with CelLytic B (Sigma), followed by centrifugation. The soluble fraction was subjected to a nickel-nitrilotriacetic acid Spin Kit (Qiagen) and further to a MicroSpin GST purification module (Amersham Biosciences). The purified protein, designated GST-mVWF73-H, was used as substrates for enzymatic assays. The molecular mass of GST-mVWF73-H was 35.7 kDa. If mADAMTS13 cleaves the expected site, the size of the N-terminal portion including the GST tag will be 28.0 kDa.

Transient Expression of mADAMTS13—The entire open reading frame (ORF) constructs with C-terminal FLAG sequence (DYKD-DDDK) were prepared for two types of mouse ADAMTS13, mADAMTS13L (GenBank™ accession number AB112362) and mADAMTS13S (GenBank™ accession number AB071302), by PCR. Each PCR product was inserted into pCAGG-neo mammalian expression vector (25). The resulting plasmids were transfected into HeLa cells using FuGENE 6 (Roche Applied Science) as described previously (16). Forty-eight hours after transfection, the media were collected and concentrated using Centricon YM-30 (Millipore). The cells together with extracellular matrix were lysed in SDS sample buffer (10 mM

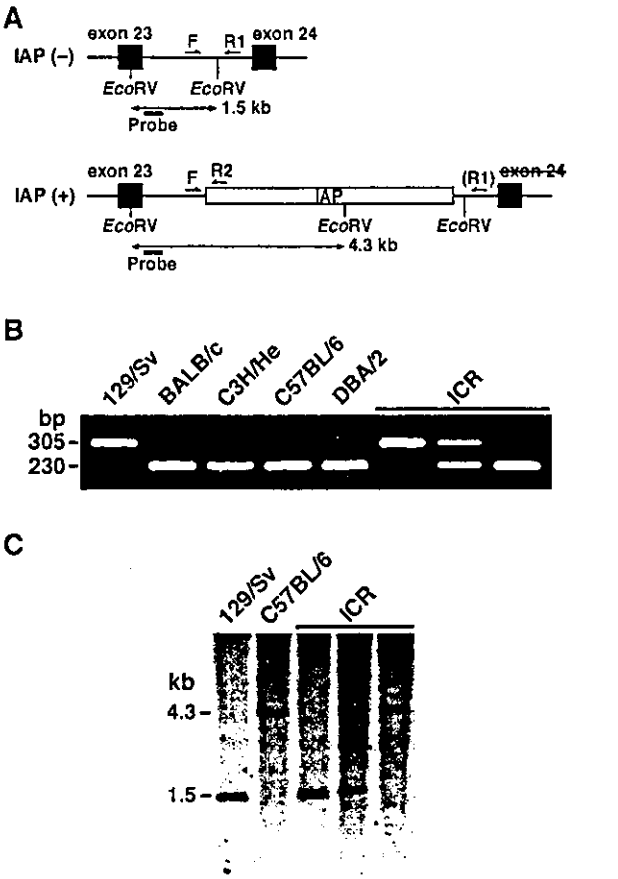

FIG. 2. **Genotyping of mouse *Adamts13*.** *A*, diagram of a segment of the *Adamts13* gene around the IAP insertion site. The sites of primers used for the genotyping PCR are indicated by *arrows*. The EcoRV fragments detected in Southern blot analysis are indicated by *double-headed arrows*. *B*, PCR analysis. In mixture of three primers, F and R1 primers generate a 305-bp product specific for the IAP-free *Adamts13* gene, whereas F and R2 primers generate a 230-bp product specific for the IAP-inserted *Adamts13* gene. *C*, Southern blot analysis. Genomic DNA from each mouse strain was digested with EcoRV and hybridized with the probe that detects a 1.5-kb fragment in the IAP-free allele and a 4.3-kb fragment in the IAP-inserted allele.

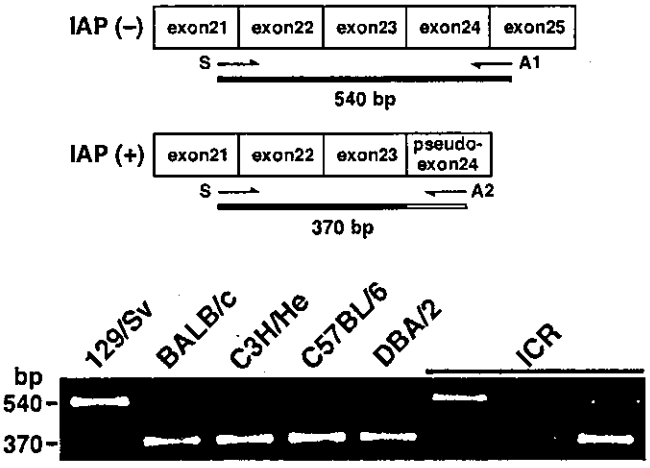

FIG. 3. **RT-PCR of *Adamts13* mRNA in liver.** PCR primers are shown as *arrows* indicating direction at their approximate locations. In combination of three primers, S and A1 primers generate a 540-bp product specific to the IAP-free transcript, whereas primers S and A2 generate a 370-bp product specific to the IAP-inserted transcript.

Tris-HCl, 2% SDS, 50 mM dithiothreitol, 2 mM EDTA, 0.02% bromphenol blue, 6% glycerol, pH 6.8).

Recombinant proteins were detected by SDS-PAGE and Western blot as described previously (16). For culture media, a rabbit anti-

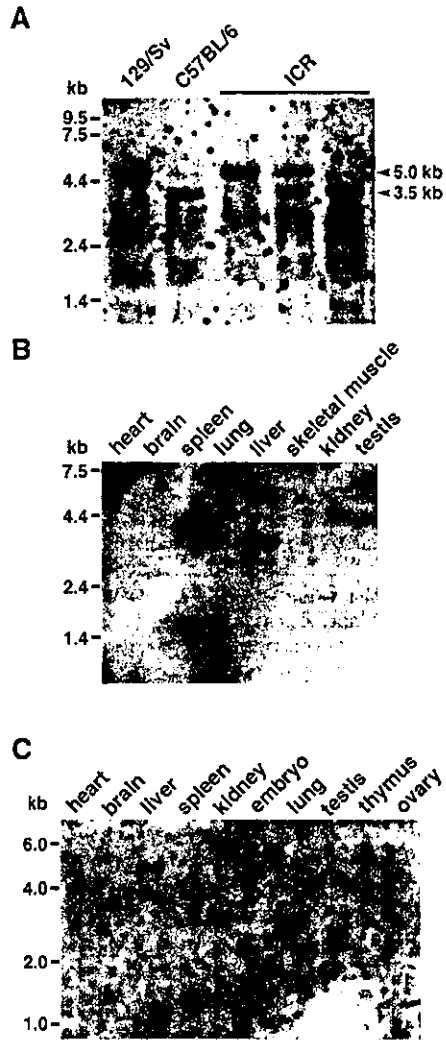

FIG. 4. **Northern blot analysis of mouse *Adamts13* mRNA.** *A*, expression of *Adamts13* mRNA in liver. Poly(A)$^+$ RNA isolated from liver of indicated strains was probed with a 1.3-kb *Adamts13* cDNA corresponding to exons 3–13. The approximate sizes of the IAP-free (5.0 kb) and the IAP chimeric (3.5 kb) transcripts are indicated by *arrowheads*. *B*, expression of *Adamts13* mRNA in tissues from BALB/c mice. *C*, expression of *Adamts13* mRNA in tissues from SwissWebster mice. The sizes of RNA markers are shown at the *left*.

mADAMTS13 polyclonal antibody (described below) and an HRP-labeled goat anti-rabbit IgG antibody (Kirkegaard & Perry Laboratories) were used for detection after SDS-PAGE under nonreducing condition. For cell lysates, an anti-FLAG M2 monoclonal antibody (Sigma) and an HRP-labeled goat anti-mouse IgG antibody (Kirkegaard & Perry Laboratories) were used for detection after SDS-PAGE under reducing condition. Chemiluminescence was developed using the Western Lighting Chemiluminescence Reagent Plus (PerkinElmer Life Sciences) and detected by an LAS-1000plus image analyzer (Fujifilm).

Preparation of Polyclonal Antibody against Mouse ADAMTS13—A polyclonal antiserum against mADAMTS13 was raised by DNA-based immunization protocols. Rabbits were immunized by intradermal injection with ~1 mg of mADAMTS13S expression plasmid at 25 sites on the back. Booster immunizations were carried out by the same protocol 3 weeks after the primary immunization. Serum was collected 3 weeks after the second immunization. The IgG fraction was then prepared by an affinity chromatography using a protein G column (Amersham Biosciences).

Enzymatic Assay—Purified GST-mVWF73-H (500 ng) was incubated with recombinant mADAMTS13L or mADAMTS13S in 40 μl of reaction buffer (5 mM Tris-HCl, 10 mM $BaCl_2$, 0.01% Tween 20, and 1 mM *p*-amidinophenylmethanesulfonyl fluoride hydrochloride, pH 8.0) at 37 °C for 1 h. The reaction was stopped by adding 10 μl of SDS sample buffer (50 mM Tris-HCl, 10% SDS, 250 mM dithiothreitol, 10 mM EDTA, 0.1% bromphenol blue, 30% glycerol, pH 6.8). The samples were sub-

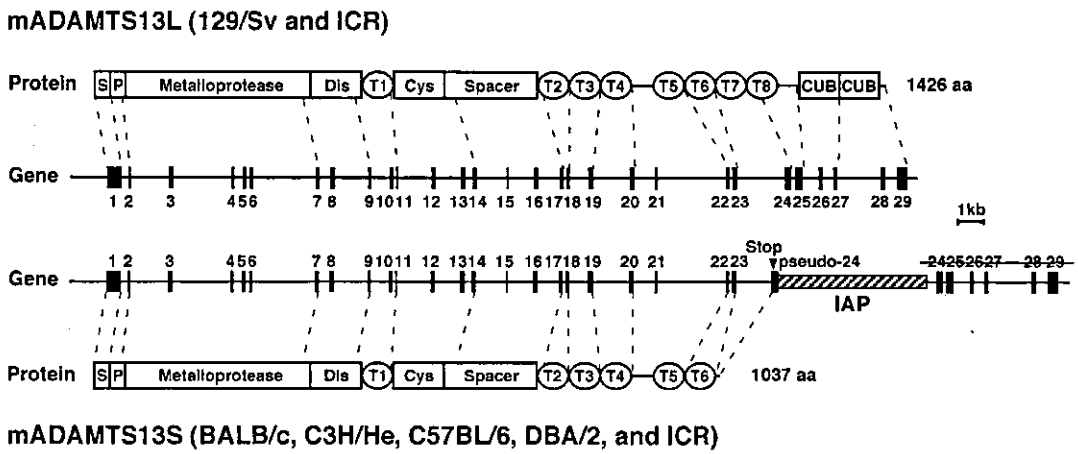

FIG. 5. **Schematic structure of two forms of the *Adamts13* genes and proteins.** Genomic and protein structures of mADAMTS13L in the 129/Sv strain and of mADAMTS13S in the BALB/c, C3H/He, C57BL/6, and DBA/2 strains are shown. The outbred ICR strain has both type alleles. The exons and introns are drawn to scale. A *hatched box* represents the IAP insertion in intron 23. *S*, signal peptide; *P*, propeptide; *Dis*, disintegrin-like domain; *T1–T8*, thrombospondin type1 motifs; *Cys*, cysteine-rich domain.

jected to Western blot using a rabbit anti-GST antibody (Molecular Probes) and an HRP-labeled goat anti-rabbit IgG antibody (Kirkegaard & Perry Laboratories) as described (24). We also analyzed the proteolytic activity of plasma from five mouse strains in the same way.

RESULTS

Identification of Adamts13 in the C57BL/6 Strain—To identify the orthologous mouse gene of human *ADAMTS13*, we performed a BLAST search in the public data base, based on the human *ADAMTS13* cDNA sequence (GenBank™ accession number AB069698, 4,284-nucleotide ORF) reported by Soejima *et al.* (8). This search led us to identify a compatible genomic sequence (GenBank™ accession number AC090008) derived from the C57BL/6 strain. This sequence was located on chromosome 2, band A3 and contained 29 conserved exons similar to human *ADAMTS13*. To obtain the cDNA to corresponding mRNA, we performed RT-PCR and 3′-RACE using poly(A)$^+$ RNA from the liver of a C57BL/6 mouse. Unexpectedly, the cDNA sequence (GenBank™ accession number AB071302) included only a 3,114-nucleotide ORF derived from 24 exons.

From a comparison between the cDNA and the genomic sequences of the C57BL/6 strain, we found a 6-kb retrovirus-like sequence in intron 23 of the *Adamts13* gene (Fig. 1). This sequence was flanked by the identical 338-bp sequence with a 6-bp (CACTAG) duplication of target site, as is often observed for retrotransposition. A BLAST search identified the insertional element as an intracisternal A-particle (IAP), which is one of the retrotransposons present at about 2,000 sites in the mouse genome (26). This insertion of IAP seemed to be responsible for loss of the original mRNA 3′-end by splicing exon 23 to pseudo-exon 24 that contains a premature stop codon.

Identification of Adamts13 in the 129/Sv Strain—To determine whether the IAP insertion into the *Adamts13* gene is common to a variety of mouse strains, we carried out PCR genotyping of five inbred and one outbred strains (Fig. 2*A*). A mixture of three primers was used for the reaction; Primers F and R1 were designed to produce a 305-bp band in the absence of IAP, and primers F and R2 were designed to produce a 230-bp band in the presence of IAP. This experiment revealed that the IAP insertion was present in the BALB/c, C3H/He, and DBA/2 strains but not in the129/Sv strain (Fig. 2*B*). The outbred ICR strain was genetically heterogeneous with respect to the IAP insertion into the *Adamts13* gene. Southern blot analysis using probes upstream of the IAP target site revealed that *Adamts13* was a single copy gene and confirmed the strain-specific insertion of IAP (Fig. 2*C*). These results implied that the *Adamts13* gene transcript of the 129/Sv mice and some ICR mice might contain residual exons lost in the other mouse strains.

To confirm this hypothesis, RT-PCR was performed using liver poly(A)$^+$ RNA from a 129/Sv mouse. The obtained sequences indicated that the *Adamts13* cDNA (GenBank™ accession number AB112362) contained a 4,281-nucleotide ORF similar to human *ADAMTS13* (4,284-nucleotide ORF). To determine the complete genomic sequence of *Adamts13* in the 129/Sv strain, we screened a 129/Sv mouse λ genomic library. Sequence analysis of positive phage clones confirmed the absence of IAP in the *Adamts13* gene. *Adamts13* in the 129/Sv strain (GenBank™ accession number AB095445) contained 29 exons like human *ADAMTS13* and spanned ~30 kb.

To examine the effect of IAP on *Adamts13* mRNA splicing, RT-PCR was performed using liver poly(A)$^+$ RNA from six mouse strains (Fig. 3). The exon 21/22-specific sense primer, the exon 24/25-specific antisense primer, and the pseudo-exon 24-specific antisense primer were mixed and used for the amplification. We detected the IAP chimeric transcript in four inbred strains with the IAP insertion. In contrast, the IAP-free transcript was observed in the 129/Sv strain. The heterogeneous expression of two types of transcripts was observed in samples from the ICR strain. To characterize the transcripts in more detail, Northern blot analysis of liver RNA was carried out using a 1.3-kb probe spanning exons 3–13 of *Adamts13* cDNA (Fig. 4*A*). The RNA was prepared from the same animals as used for the Southern blot analysis. An ~3.5-kb mRNA corresponding to the size of IAP chimeric transcript was detected in the C57BL/6 and the ICR strains. The IAP-free transcript of ~5.0 kb was observed in the 129/Sv and the ICR strains.

Thus, these results clearly indicate the presence of two types of mouse *Adamts13* in a strain-specific manner (Fig. 5). *Adamts13* of the 129/Sv strain encodes an ADAMTS13 protein containing 1,426 amino acid residues with the same domain structure as hADAMTS13, designated mADAMTS13L. *Adamts13* of the BALB/c, C3H/He, C57BL/6, and DBA/2 strains encodes the shorter ADAMTS13 protein including only 1,037 amino acid residues, designated mADAMTS13S. In this protein, the C-terminal two TSP1 and two CUB domains are replaced with the 16-amino acid sequence, ALVWEAAPTFAVTRWR, derived from the IAP. The outbred ICR strain carries either the IAP-free or IAP-inserted allele or both.

Expression of the Adamts13 mRNA in Mouse Tissues—To study the expression pattern of the mouse *Adamts13* gene, we analyzed Northern blots containing poly(A)$^+$ RNA from various tissues of the BALB/c and the Swiss Webster strains. As shown

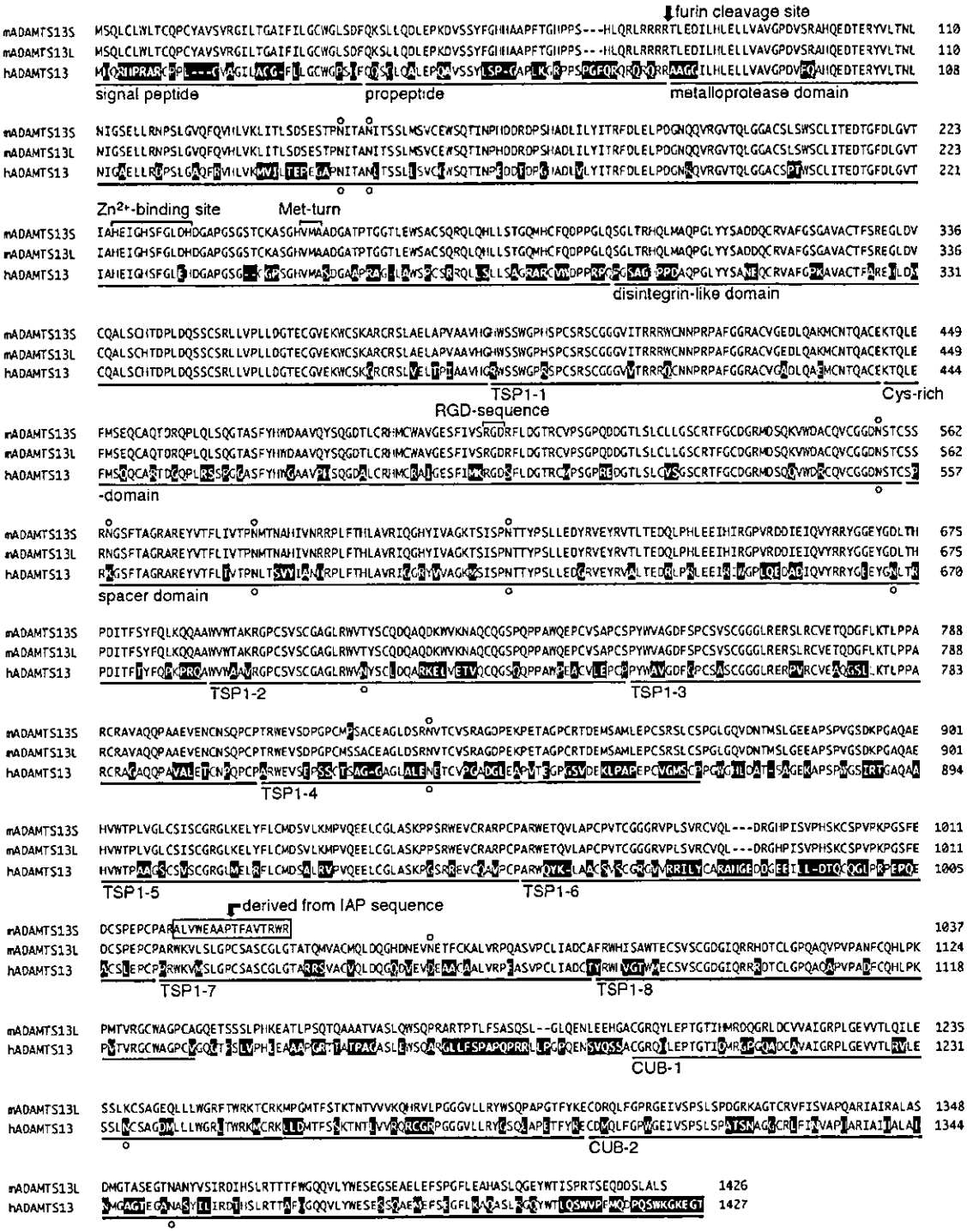

FIG. 6. **Alignment of deduced amino acid sequences of mADAMTS13 and hADAMTS13.** Sequences are represented with the *single-letter code*, and residues that differ from mADAMTS13L are *shaded*. Each structural domain is *underlined*. The predicted furin cleavage site (R*X*(K/R)R) is marked with an *arrow*. The IAP-derived 16 amino acid residues in mADAMTS13S are *boxed*. *Open circles* indicate the potential *N*-glycosylation sites.

in Fig. 4 (*B* and *C*), *Adamts13* mRNA in both strains was exclusively observed in the liver, suggesting that mADAMTS13 is primarily synthesized in the liver, similar to hADAMTS13. A single transcript of 3.5 kb was expressed in liver of the BALB/c strain with the IAP insertion. In contrast, two transcripts of 5.0 and 3.5 kb were detected in liver of the outbred Swiss Webster strain, suggesting that this strain may carry two types of alleles, like the ICR strain. Both SwissWebster and ICR strains are derived from a colony of Swiss mice.

Comparison of the Deduced Amino Acid Sequences of mADAMTS13 and hADAMTS13—The deduced amino acid sequences of mouse and human ADAMTS13 were aligned (Fig. 6). The overall sequence identity between mADAMTS13L and hADAMTS13 was ~70%. The highest identity (>80%) was observed in the disintegrin-like (81%), TSP1–1 (89%), cysteine-rich (80%), and TSP1–8 (83%) domains, whereas relatively low conservation (<60%) was observed in the signal peptide (43%), propeptide (52%), TSP1–4 (46%), and TSP1–6 (40%) domains. mADAMTS13L contained eight potential *N*-glycosylation sites, six of which were conserved in hADAMTS13. mADAMTS13L also included several motifs characteristic for each domain of hADAMTS13, such as a furin cleavage sequence at the end of

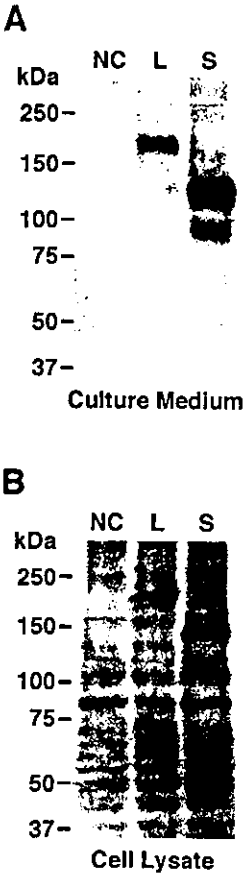

FIG. 7. **Transient expression of recombinant mADAMTS13.** *A*, mADAMTS13 in the culture medium. HeLa cells were transfected with plasmids encoding mADAMTS13L (*L*) and mADAMTS13S (*S*). The concentrated culture media were analyzed by Western blot with an anti-mADAMTS13 antibody under nonreducing conditions. *B*, mADAMTS13 in the cell lysate. The cell lysates including extracellular matrixes were analyzed by Western blot with an anti-FLAG antibody under reducing condition. *NC* is the culture medium or the lysate of untransfected cells. The size of protein markers is indicated at the *left*. The small size difference of recombinant enzymes in medium and cell lysates was due to the difference of electrophoretic condition. The faster migrating bands seen in medium and cell lysates expressing mADAMTS13S may result from proteolysis during cell culture. The typical result of three experiments is shown.

the propeptide, a zinc-binding site in the metalloprotease domain, and an RGD sequence in the cysteine-rich domain. The sequences of mADAMTS13L and mADAMTS13S were almost identical, except for the deletion of C-terminal regions.

Expression and Enzymatic Activity of Recombinant mADAMTS13L and mADAMTS13S—We transiently expressed the mADAMTS13L and mADAMTS13S proteins in HeLa cells. Western blot analysis using a polyclonal antibody against mADAMTS13 revealed that both were secreted into the culture media (Fig. 7*A*). Transient expression of mADAMTS13L produced an immunoreactive band of ~200 kDa, and mADAMTS13S exhibited a 130-kDa band. The level of mADAMTS13S in the medium was almost 10-fold higher than that of mADAMTS13L. This was not due to a preferential accumulation of mADAMTS13L on the cell surface or the extracellular matrix, because a relatively high amount of mADAMTS13S was also observed in the cell lysates (Fig. 7*B*). It was conceivable that mADAMTS13S was effectively synthesized in HeLa cells compared with mADAMTS13L in our experimental conditions. Whether mADAMTS13S is also preferentially expressed *in vivo* remains unknown. Further analysis is required to determine the plasma levels of mADAMTS13L and mADAMTS13S in mice.

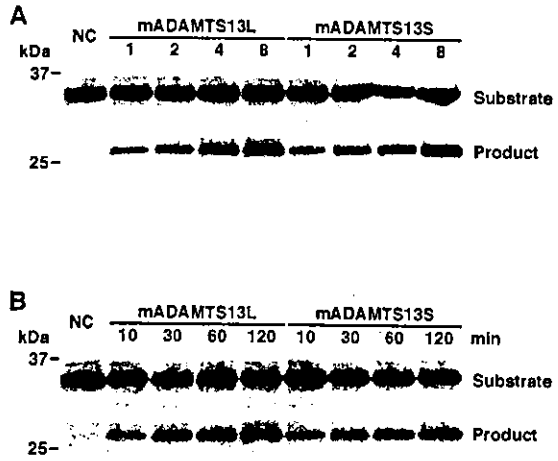

FIG. 8. **Enzymatic activity of recombinant mADAMTS13.** *A*, cleavage of GST-mVWF73-H by serial dilutions of mADAMTS13. GST-mVWF73-H was incubated with recombinant mADAMTS13L or mADAMTS13S at 37 °C for 1 h. A negative control reaction using the culture medium of untransfected cells (NC) was also performed simultaneously. The products were analyzed by Western blot using an anti-GST antibody. The *numbers 1, 2, 4,* and *8* indicate relative amounts of mADAMTS13L and mADAMTS13S in the reaction mixtures. The typical result of three experiments is shown. *B*, time course of GST-mVWF73-H cleavage by mADAMTS13. GST-mVWF73-H was incubated with recombinant mADAMTS13L or mADAMTS13S for the indicated time at 37 °C. The reaction mixtures contained the equivalent amounts of the recombinant enzyme. Products were analyzed by Western blot using an anti-GST antibody. The typical result of three experiments is shown.

The VWF cleaving activities of recombinant proteins were measured by the degradation of the specific recombinant substrate, GST-mVWF73-H. The relative concentration of recombinant mADAMTS13 in the culture medium was determined by chemiluminescent intensities on Western blot, and equal amounts were used for the enzymatic assay. The substrate, GST-mVWF73-H, was incubated with serial dilutions of the culture medium, and the cleavage product including the N-terminal GST tag was visualized by Western blot using anti-GST (Fig. 8). When the substrate was incubated with the medium of mADAMTS13L-transfected cells, a band appeared with the expected size of the N-terminal portion (28 kDa) in a concentration-dependent manner, indicating the cleaving activity of recombinant mADAMTS13L (Fig. 8*A*). No degradation was observed after the incubation of GST-mVWF73-H with the medium from untransfected cells. The cleaved band was also detected after incubation with the mADAMTS13S culture medium, and the chemiluminescent intensities of the product bands were almost equal to those obtained by mADAMTS13L (Fig. 8*A*). We confirmed that the degradation of GST-mVWF73-H by mADAMTS13 was also time-dependent, and the rate of the product formation by mADAMTS13S was similar to that by mADAMTS13L (Fig. 8*B*).

The VWF Cleaving Activity of Mouse Plasma—To examine the ADAMTS13 activity in plasma from various mouse strains, we collected plasma samples from five strains and carried out the enzymatic assay using GST-mVWF73-H. As shown in Fig. 9, plasma from all strains cleaved GST-mVWF73-H. Comparison of the product levels did not reveal a significant difference among strains. This suggested that the IAP insertion into the *Adamts13* gene does not affect the *in vitro* cleavage of GST-mVWF73-H by plasma.

DISCUSSION

In this study, we identified two isoforms of the mouse *Adamts13* gene that result from the strain-specific insertion of

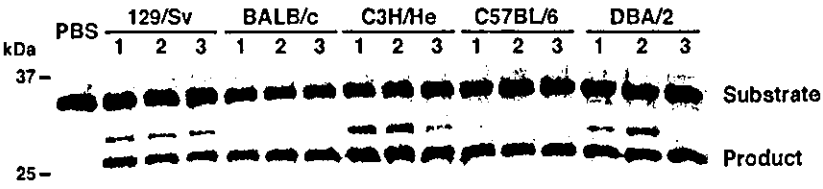

FIG. 9. **Cleavage of GST-mVWF73-H by mouse plasma.** GST-mVWF73-H was incubated with plasma samples from mice with (BALB/c, C3H/He, C57BL/6, and DBA/2) or without (129/Sv) the IAP insertion in the *Adamts13* gene. The products were analyzed by Western blot using an anti-GST antibody. The results from three animals/strain are shown.

an IAP-retrotransposon. The IAP-free *Adamts13* gene contained 29 exons, and the deduced protein sequence included 1,426 amino acid residues with the same domain organization as hADAMTS13. In contrast, the IAP-inserted *Adamts13* gene contained only 24 exons encoding 1,037 amino acids having a truncated C terminus.

The inserted IAP is one of the endogenous transposable elements, which is closely related to retroviruses and transposed via the reverse transcription of an RNA intermediate (26, 27). The IAP element contains two long terminal repeats with the signals for the initiation/regulation of transcription and for the polyadenylation of transcripts (28). IAP insertions into introns have been shown to cause formation of chimeric transcripts (29–32), similar to our findings in the *Adamts13* gene. We noted that the presence of IAP in the *Adamts13* gene induces the appearance of a cryptic splicing site followed by a premature in-frame stop codon and a polyadenylation signal derived from the IAP long terminal repeat. As a result, the insertion leads to replacement of the last 405 amino acid residues corresponding to two TSP1 motifs and two CUB domains with the IAP-encoded 16 amino acid residues.

Northern blot and RT-PCR analyses confirmed that the IAP chimeric short transcript (3.5 kb) and the IAP-free long transcript (5 kb) were expressed in a strain-specific manner. Both types of transcripts were specifically expressed in the liver, consistent with expression of the human *ADAMTS13* gene. It should be noted that the IAP insertion could not completely abolish the formation of mADAMTS13L mRNA. The RT-PCR products (540-bp; Fig. 3) characteristic of mADAMTS13L mRNA were also detectable in the strains with the IAP insertion when using a large amount of template (data not shown). A small amount of mADAMTS13L protein may be expressed in mice with the IAP-inserted *Adamts13* gene such as the BALB/c, C3H/He, C57BL/6, and DBA/2 strains. Incidentally, the RT-PCR and 3′-RACE data did not show any splicing variants that encoded mADAMTS13S-like protein in the IAP-free strains.

Recently, we developed a novel recombinant substrate, GST-VWF73-H, to measure hADAMTS13 activity (24). GST-VWF73-H is a partial region of human VWF flanked by GST and His_6 tags. Because of difficulty in isolating VWF from mouse plasma, we have also prepared the recombinant substrate, GST-mVWF73-H, based on the mouse VWF cDNA sequence. Both mouse and human plasma efficiently cleaved GST-mVWF73-H and produced a fragment of the expected size. Mouse plasma also cleaved the substrate for hADAMTS13, GST-VWF73-H (data not shown).

Both recombinant mADAMTS13L and mADAMTS13S were secreted into the culture medium of HeLa cells. This result indicates that the IAP insertion does not abolish secretion of mADAMTS13 from cells. The recombinant mADAMTS13L and mADAMTS13S cleaved GST-mVWF73-H with nearly the same efficiency. Similarly, a deletion mutant of hADAMTS13 in mimicry of mADAMTS13S was also secreted efficiently from HeLa cells and cleaved GST-VWF73-H with normal activity (data not shown). In previous reports, we and others found that deletion mutants of hADAMTS13 devoid of the C-terminal TSP1 motifs and CUB domains retained VWF cleaving activity (21, 22). Therefore, our current observation on mouse and human recombinant proteins was consistent with these previous studies. Moreover, the plasma VWF cleaving activities in mice were also comparable among the strains with or without the IAP insertion in the *Adamts13* gene. The C-terminal two TSP1 motifs and two CUB domains of mADAMTS13 may contribute to activity but are not essential for the VWF cleavage, at least *in vitro*.

The fact that several common strains of mice have a naturally truncated form of ADAMTS13 allows us to hypothesize that the truncated domains are not necessary *in vivo*. However, several mutations in TSP1–7, TSP1–8, CUB-1, and CUB-2 domains of hADAMTS13 were reported to associate with congenital thrombotic thrombocytopenic purpura (15, 17–20). It is still unclear whether these mutants are secreted from cells, as is the case with mADAMTS13S. To date, two mutations, R1123C and 4143insA, were characterized by expression analysis, and both impaired secretion of the enzyme from cells (19, 20). The C-terminal mutations found in thrombotic thrombocytopenic purpura patients may influence their synthesis or secretion.

Bernardo *et al.* (33) reported that several short peptides within the regions from TSP1–6 to the C terminus of hADAMTS13 block VWF cleavage on the endothelial cell surface under flow conditions. This finding suggests an important role for the C-terminal domains *in vivo*. Although our results clearly show that the mouse has managed without full-length ADAMTS13, the relative importance of ADAMTS13 for regulation of VWF activity may be different between human and mouse. A gene targeting technique of mouse *Adamts13* will help to clarify the physiological contribution of mADAMTS13.

Acknowledgments—We thank Yuko Nobe, Yoko Tokunaga (National Cardiovascular Center Research Institute), Noriko Mimura, and Arisa Maeyashiki (The Chemo-Sero-Therapeutic Research Institute) for technical assistance.

REFERENCES

1. Furlan, M. (1996) *Ann. Hematol.* **72,** 341–348
2. Sadler, J. E. (1998) *Annu. Rev. Biochem.* **67,** 395–424
3. Dent, J. A., Galbusera, M., and Ruggeri, Z. M. (1991) *J. Clin. Invest.* **88,** 774–782
4. Federici, A. B., Bader, R., Pagani, S., Colibretti, M. L., De Marco, L., and Mannucci, P. M. (1989) *Br. J. Haematol.* **73,** 93–99
5. Kalafatis, M., Takahashi, Y., Girma, J. P., and Meyer, D. (1987) *Blood* **70,** 1577–1583
6. Moake, J. L., Rudy, C. K., Troll, J. H., Weinstein, M. J., Colannino, N. M., Azocar, J., Seder, R. H., Hong, S. L., and Deykin, D. (1982) *N. Engl. J. Med.* **307,** 1432–1435
7. Moschcowitz, E. (1924) *Proc. N. Y. Pathol. Soc.* **24,** 21–24
8. Soejima, K., Mimura, N., Hirashima, M., Maeda, H., Hamamoto, T., Nakagaki, T., and Nozaki, C. (2001) *J. Biochem.* **130,** 475–480
9. Gerritsen, H. E., Robles, R., Lämmle, B., and Furlan, M. (2001) *Blood* **98,** 1654–1661
10. Fujikawa, K., Suzuki, H., McMullen, B., and Chung, D. (2001) *Blood* **98,** 1662–1666
11. Dent, J. A., Berkowitz, S. D., Ware, J., Kasper, C. K., and Ruggeri, Z. M. (1990) *Proc. Natl. Acad. Sci. U. S. A.* **87,** 6306–6310
12. Furlan, M., Robles, R., and Lämmle, B. (1996) *Blood* **87,** 4223–4234
13. Tsai, H. M. (1996) *Blood* **87,** 4235–4244
14. Zheng, X., Chung, D., Takayama, T. K., Majerus, E. M., Sadler, J. E., and Fujikawa, K. (2001) *J. Biol. Chem.* **276,** 41059–41063
15. Levy, G. G., Nichols, W. C., Lian, E. C., Foroud, T., McClintick, J. N., McGee, B. M., Yang, A. Y., Siemieniak, D. R., Stark, K. R., Gruppo, R., Sarode, R., Shurin, S. B., Chandrasekaran, V., Stabler, S. P., Sabio, H., Bouhassira, E. E., Upshaw, J. D., Jr., Ginsburg, D., and Tsai, H. M. (2001) *Nature* **413,** 488–494